

Heat disproportionately kills young people: evidence from wet-bulb temperature in Mexico

Andrew J. Wilson^{†1,2,3}, R. Daniel Bressler^{†*4,5,3}, Catherine Ivanovich^{5,6}, Cascade Tuholske⁷, Colin Raymond^{8,9}, Radley M. Horton^{5,6}, Adam Sobel^{5,6,10}, Patrick Kinney¹¹, Tereza Cavazos¹², and Jeffrey G. Shrader^{4,5,3}

¹Center on Food Security and the Environment, Stanford University

²Global Policy Laboratory, Stanford University

³Center for Environmental Economics and Policy, Columbia University

⁴School of International and Public Affairs, Columbia University

⁵Climate School, Columbia University

⁶Department of Earth and Environmental Sciences, Columbia University

⁷Department of Earth Sciences, Montana State University

⁸Joint Institute for Regional Earth System Science and Engineering, University of California, Los Angeles

⁹NASA Jet Propulsion Laboratory

¹⁰Department of Applied Physics and Applied Mathematics, Columbia University

¹¹School of Public Health, Boston University

¹²Department of Physical Oceanography, CICESE, B.C., Mexico

[†]Equal contribution

*Correspondence: rdb2148@columbia.edu

Published 6 Dec 2024 in *Science Advances*.

Abstract

Recent studies project that temperature-related mortality will be the largest source of damage from climate change, with particular concern for the elderly whom it is believed bear the largest heat-related mortality risk. We study heat and mortality in Mexico, a country that exhibits a unique combination of universal mortality microdata and among the most extreme levels of humid heat. Combining detailed measurements of wet-bulb temperature with age-specific mortality data, we find that it is younger people who are particularly vulnerable to heat: people under 35 years old account for 75% of recent heat-related deaths and 87% of heat-related lost life years while those 50 and older account for 96% of cold-related deaths and 80% of cold-related lost life years. We develop high-resolution projections of humid heat and associated mortality and find that under the end-of-century SSP 3-7.0 emissions scenario, temperature-related deaths shift from older to younger people. Deaths among under-35-year-olds increase 32% while decreasing by 33% among other age groups.

1 Introduction

Historically, temperature exposure has caused a large number of premature deaths [1–3]. Heat-related mortality is expected to increase under climate change [4–27]. As the evidence base has grown, multiple studies have found that the elderly are especially vulnerable to heat [6, 11, 14, 17, 18, 28, 29]. Furthermore, many other studies have expressed particular concern for joint heat and humidity extremes, given the importance of perspiration for human thermoregulation [30–36].

In this study, we explore the relationship between humid heat and mortality in Mexico, a country that exhibits a unique combination of rich age-specific universal mortality microdata and among the most extreme historical humid heat exposures. We find that historically, the majority of heat-related mortality in Mexico has been concentrated among younger people: 75% of heat-related deaths and 87% of heat-related lost life years occur among those under 35 years old. By contrast, the vast majority of cold-related mortality is concentrated among older people: 98% of cold-related deaths and 90% of cold-related lost life years occur among those over 35, with the majority of cold-related deaths occurring among individuals older than 70 years. We then develop projections of humid heat and associated outcomes to assess the future implications of these findings. As in other studies, we find that climate change is expected to increase heat-related mortality while decreasing cold-related mortality. However, we uncover an important source of future climate-driven inequality: the disproportionate impact of heat and cold across age groups reallocates the temperature-related mortality burden from the elderly (who are more impacted by cold) to the young (who are more impacted by heat). This has important implications for understanding the distributional impacts of climate change and for developing effective policies to adapt to these impacts.

2 Methods

Our insights into the effect of humid heat across the lifespan result from a combination of four elements: (1) station-level wet-bulb temperature estimates; (2) high-quality, age-specific, population-wide mortality microdata; (3) a statistical method that resolves age-specific heterogeneity in temperature vulnerability; and (4) realistic, granular projections of humid heat under climate change

41 across our study area.

42 First, we study the effect of *wet-bulb temperature* on mortality. While multiple metrics exist to
43 measure humid heat stress [37], wet-bulb temperature has been identified as an important metric
44 for understanding the impact of heat on human health because it accounts for the critical role of
45 sweat evaporation—the primary mechanism by which the human body cools itself—in maintaining
46 homeostasis under heat exposure [36, 38]. Under high humidity, sweating efficiency decreases [37,
47 39, 40]. When ambient wet-bulb temperature exceeds human skin temperature (at around 35°C),
48 humans can no longer dissipate heat into the environment and are thus physically incapable of
49 survival when exposed for a sufficient length of time [30, 32, 33]. In practice, experimental evidence
50 has shown that heat stress can become uncompensable at wet-bulb temperatures of 31°C or lower
51 [34, 35]. Under high emissions scenarios, increasing humid heat stress is projected to cause some
52 regions to become uninhabitable for parts of the year without artificial cooling [33]. Despite the
53 importance of both heat and humidity for human thermoregulation, most empirical studies on
54 temperature-related mortality have focused on dry-bulb temperature, which does not account for
55 humidity. Hundreds of papers have been written on the mortality impact associated with dry-
56 bulb temperature [4, 8]. One review found only nine papers that assessed the role of humid heat
57 on mortality [31], and there remain important gaps in our understanding of the population-wide
58 health impacts of humid heat [36].

59 Second, our study leverages precise historical data on both mortality and temperature exposure.
60 Mexico’s high-quality vital statistics microdata includes a record of each death occurring in the
61 country since 1998. Crucially, these microdata also contain information on age at death, allowing us
62 to assess age-specific heterogeneity in the relationship of heat and mortality with more precision than
63 prior literature, which has focused on broader age groups or on effects only among the elderly [6, 12,
64 36, 41, 42]. Over the 22 years from 1998 to 2019. We choose to end our study period in 2019, before
65 the COVID-19 pandemic. The data contain information on the day and municipality—Mexico’s
66 second-order administrative unit, numbering around 2,400 across the country—of occurrence of
67 13.4 million deaths over more than 21 million municipality–days. We combine these records with
68 station-level, sub-daily measurements of dry-bulb temperature, humidity, and air pressure, which we

69 use to develop estimates of local daily mean wet-bulb temperature [43]. This is important because
70 we find evidence that weather reanalysis data products such as ERA5-Land do not reproduce the
71 most extreme humid heat events observed by Mexico’s station network (see Figure S13). Mexico’s
72 heterogeneous climate and rich public vital statistics records make it an ideal setting for determining
73 the impact of humid heat exposure on premature mortality. Mexico is one of the most climatically
74 diverse countries in the world, with the fourth largest number of Köppen climate zones (see Figure
75 S14). It is located in the subtropics and tropical regions, has a wide variety of elevations, is located
76 between two oceans, and experiences substantial seasonal variation, including the North American
77 monsoon. The low correlation between air temperature and humidity observed throughout many
78 areas of Mexico [36] allows extreme dry and humid heat events to take place on separate days within
79 the same location, facilitating the investigation of the distinct impacts of these two extremes.
80 Most existing studies have assessed temperature-mortality relationships in cooler, higher-income
81 countries [30, 36] that have never experienced humid heat extremes. Mexico, by contrast, has
82 experienced among the highest wet-bulb temperatures ever recorded, particularly in coastal regions
83 [32]. Substantial populations are also exposed to these diverse climates across the country (see
84 Figure S14).

85 Third, we estimate an age-specific exposure relationship between excess mortality and daily
86 average wet- and dry-bulb temperature. Our empirical model leverages current best practices to
87 isolate causal impacts of temperature on excess mortality [1, 6]. We investigate effects over a set
88 of distributed lags to capture the dynamic effects of temperature on health, including harvesting—
89 when “deaths are occurring only a few days early among persons who were already dying” [44]—and
90 delayed mortality responses. Our model flexibly captures differences in impacts from cold, moderate,
91 and hot temperature exposures and includes control variables to account for potential confounders,
92 including seasonality and time trends. We identify effects based on otherwise random changes in
93 weather across days within a given municipality, such that a municipality experiencing mild weather
94 acts as the “control group” for itself during more extreme weather, eliminating confounding spatial
95 variation. Lastly, we flexibly adjust for daily precipitation to ensure that the effects of temperature
96 are not operating via rainfall. Importantly, our statistical model allows the minimum mortality

97 temperature (MMT) to vary by age group. We find that different age groups experience minimum
98 mortality at substantially different temperatures: individuals in their 70s experience minimum
99 mortality at temperatures nearly 10°C higher than individuals in their 20s for both dry-bulb and
100 wet-bulb temperatures (see Figure S11). See Section A.2 for further details on the model and
101 estimation procedure.

102 Finally, we develop fine-scale projections of dry and humid heat through the end of the century
103 to project changes in mortality across age groups as the climate warms. We retrieve statisti-
104 cally down-scaled temperature, humidity, and precipitation projections through the end of the cen-
105 tury [45] across the greenhouse gas emissions associated with four Shared Socioeconomic Pathways
106 (SSPs) [46]; calculate wet-bulb temperature; and bias correct the dry-bulb temperature, wet-bulb
107 temperature, and precipitation projections against historical station and reanalysis data [47, 48]
108 using percentile mapping. This approach allows us to best match the spatial distribution of the
109 available human health data, as well as to capture the variability in climate and terrain throughout
110 Mexico, essential to reproducing dry and humid heat extremes [49]. For additional details, see
111 Section A.1.2.

112 **3 Results**

113 Figure 1 shows the effect of exposure to a single day at the indicated wet-bulb temperature on
114 mortality risk for different age groups. For instance, the under-5 exposure–response function implies
115 that when an individual under 5 years of age experiences one day with average wet-bulb temperature
116 of 27°C, their risk of mortality increases by 45% relative to if they had experienced one day with
117 an average wet-bulb temperature of 13°C. (For policymakers, numerical values for the estimated
118 additional number of deaths per person for different temperature exposures are shown in Table S1.)
119 Figure 2 (left panel) combines the age-specific vulnerability to heat and cold (shown in Figure 1 top
120 panel) along with the frequency with which those temperatures occur (shown in Figure 1 bottom
121 panel) to quantify the total annual number of temperature-related deaths associated with exposure
122 to temperature broken down into one-degree temperature bins and broken out by age-group during

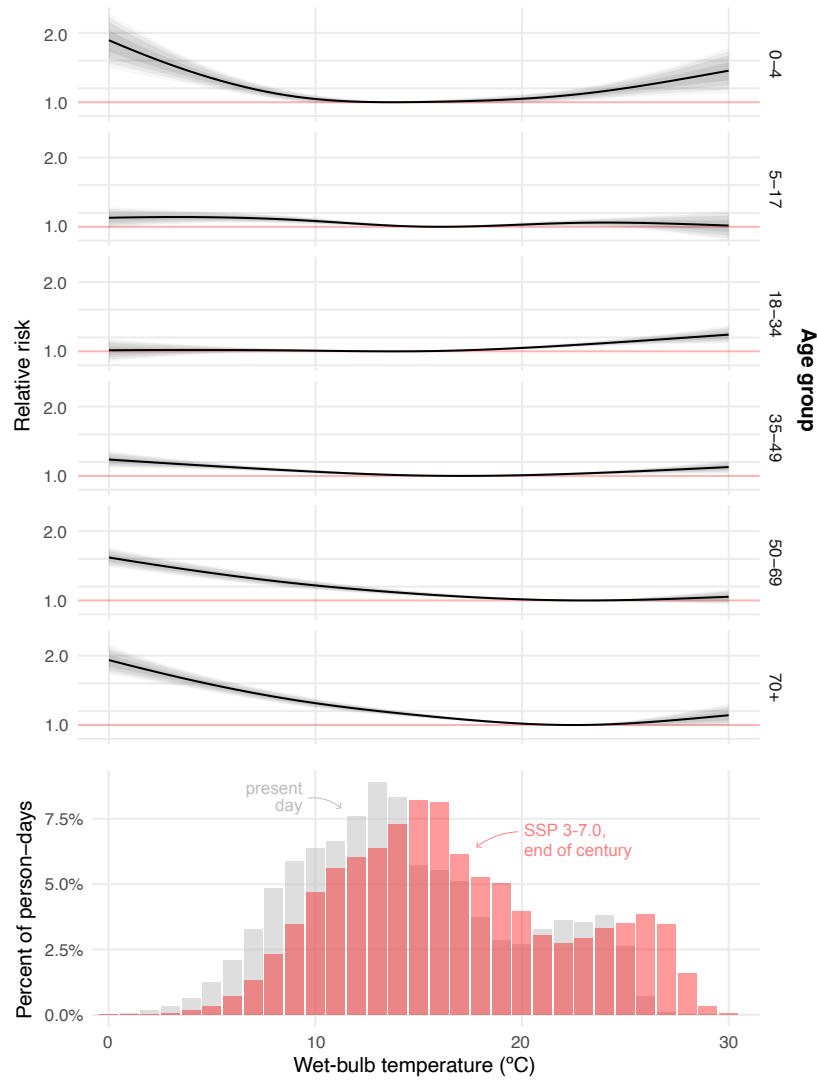


Figure 1: Relationships between mortality risk and exposure to wet-bulb temperature by age group in Mexico

The top panels show the change in relative mortality risk (y -axis) caused by exposure to one day of the indicated average daily wet-bulb temperatures (x -axis) across age groups. The bottom panel shows the distribution of daily average wet-bulb temperatures in Mexico throughout our sample period as well as the ensemble mean of projected temperature distribution at the end of the century (2083–2099) under the SSP 3-7.0 GHG emission scenario. Shaded bands around the functions in the top panels indicate 95, 90, 80, and 50% confidence intervals. Absolute changes in mortality for both wet- and dry-bulb temperature are shown in Figure S1, and coefficient estimates for absolute mortality changes are shown in Table S1.

123 our historical data period. In Figure 3, points labeled “Historical” aggregate this data to quantify
 124 the total annual number of heat and cold-related deaths by age group. These values combine age-
 125 specific vulnerability to heat and cold (shown in the top panels of Figure 1) with the frequency
 126 with which those temperatures occur (shown in the bottom row of Figure 1).

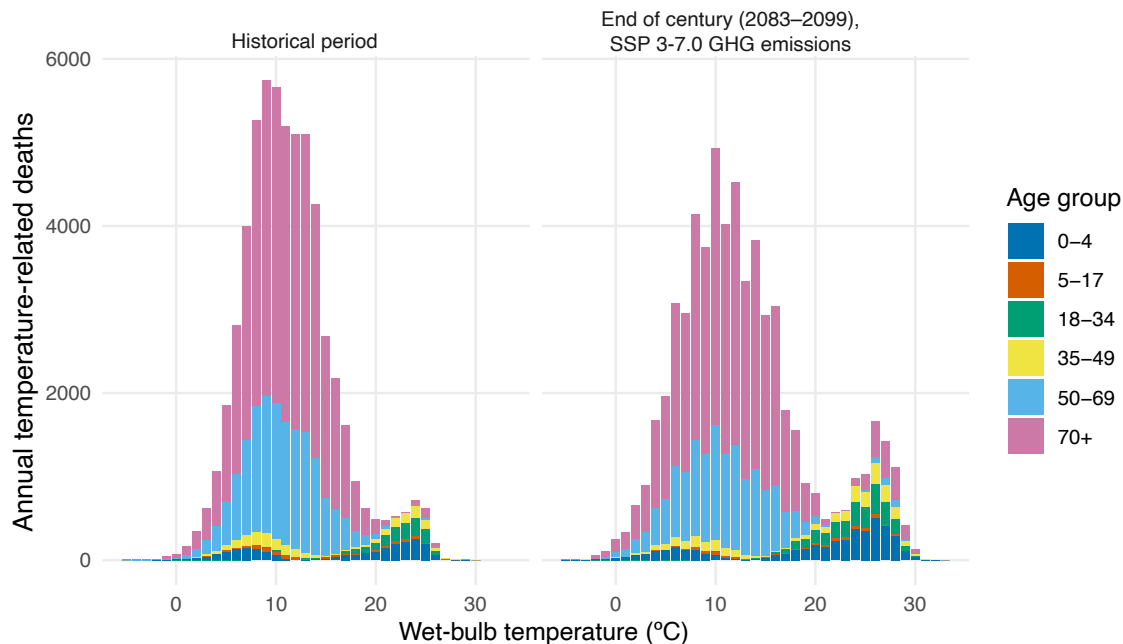


Figure 2: Historical and projected annual temperature-related deaths in Mexico

The panels show average annual temperature-related deaths resulting from exposure to days with the average wet-bulb temperatures shown on the x -axis during the historical period (left panel) and at the end of the century (2083–2099) under the SSP 3-7.0 GHG emission scenario (right panel) across six age groups in Mexico. The figure shows mean projected deaths; see Figure 3 for projections with uncertainty.

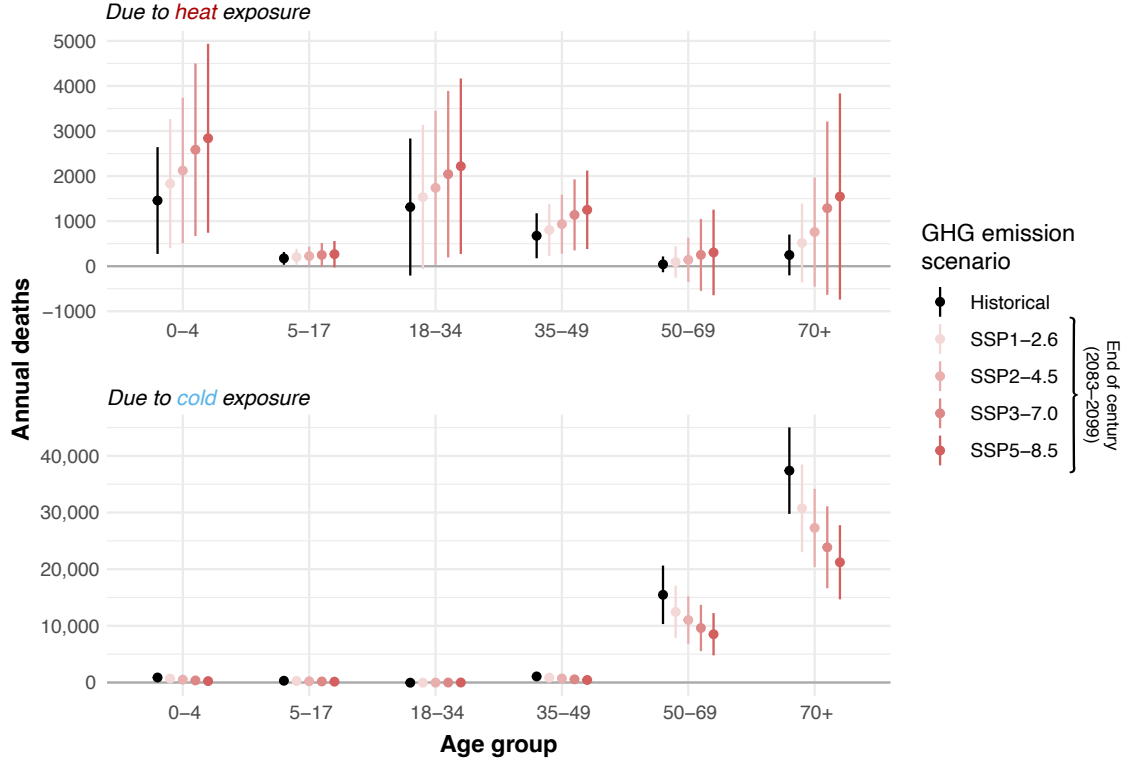


Figure 3: Historical and projected annual deaths due to heat (top panel) and cold exposure (bottom panel) by age group

The figure depicts the average annual number of deaths attributed to heat and cold exposure in Mexico historically and under wet-bulb temperatures prevailing at the end of the century in four greenhouse gas emission scenarios. Whiskers above and below each estimate depict 95% confidence intervals net of both econometric and climate uncertainty. Note that the range of the y -axis in the bottom panels is roughly eight times the range of the y -axis in the top panels.

127 Consistent with past literature on temperature-related mortality in Mexico [28, 50], we find
 128 that cold is historically associated with more deaths than heat across the whole population: cold
 129 causes 14 times more deaths than heat, as shown in Figure 3. However, this masks important
 130 heterogeneity across age groups. While cold-related mortality is concentrated among the old, heat-
 131 related mortality is concentrated among the young. For individuals under 35, heat causes 2.6 times
 132 more deaths than cold (Figure 3, top panel). Whereas for individuals 35 and older, cold causes
 133 56 times more deaths than heat (Figure 3, bottom panel). 98% of cold-related deaths occurred

134 among those 35 and older, with 28% of such deaths occurring among those 50 to 70 and 68%
135 occurring among those 70 and older. In contrast 75% of heat-related deaths occurred among under-
136 35-year-olds (the distributions of these proportions are shown in Figure S5). This contrasts with
137 the previous literature, which has found that both cold and heat-related mortality impacts are
138 concentrated among elderly people.

139 When considering lost life years, which accounts for the fact that younger individuals have on
140 average more remaining life than older individuals, the outsized impact of heat on younger age
141 groups becomes even more pronounced (Figure 4): those under 35 years old account for 87% of life
142 years lost due to recent heat exposure, whereas those 50 and older account for 80% of life years lost
143 to recent cold exposure.

144 We find that these results around the concentration of the heat-related mortality burden among
145 the young and the cold-related mortality burden among the old are robust whether we use wet-
146 or dry-bulb temperature as our metric of exposure (as shown in Figures S1, S2, S3, S4, and S5).
147 Importantly, though, nearly all historical exposures—even in our context—are below theoretically
148 uncompensable humid heat levels [34, 51].

149 The right panel of Figure 2 and the red points and whiskers in Figure 3 show our projections
150 for the number of annual deaths at the end of the century broken down by age group. These
151 projected deaths do not account for potential future adaptation or population changes, but rather
152 describe the effect of projected future temperatures on mortality given historical socioeconomic,
153 institutional, and adaptation conditions. Climate change is projected to cause more heat-related
154 mortality and less cold-related mortality across all age groups. Cold-related mortality continues to
155 be concentrated among individuals 35 and older—with the impact especially pronounced on indi-
156 viduals 70 or older—while heat-related mortality continues to be concentrated among individuals
157 under 35 years old. However, as hot days become more frequent and cold days become less frequent,
158 the overall temperature-related mortality burden shifts towards the young and away from the old.
159 Older individuals continue to suffer disproportionately from cold-related mortality, but cold days
160 are comparatively less frequent. Those under 35 suffer disproportionately from increasing heat,
161 with premature mortality especially concentrated in the under-5 and 18–34 age groups.

162 Figures 3 and S6 show the projected percent change in age group temperature-related deaths at
163 the end of the century across four different greenhouse gas emission scenarios, ranging from a rapid
164 decarbonization scenario (SSP 1-2.6) to a very high emissions scenario (SSP 5-8.5). All results
165 are relative to historical temperature-related deaths. These figures show that the age structure
166 of mortality burdens in Figure 2 holds more generally across low, medium, and high emissions
167 scenarios. In all scenarios, climate change shifts the risk of temperature-related mortality toward
168 those under 35 and away from those 50 and older. Under the SSP 3-7.0 emission scenario, we project
169 a 32% increase in temperature-related deaths among under-35-year-olds driven by an increase in
170 heat-related mortality, and a 33% decrease among those 35 and older driven by a decrease in cold-
171 related mortality (the distribution of these estimates of percent changes in overall temperature-
172 related mortality are shown in Figures S6 and S7).

173 Previous research has shown that dry-bulb temperature-related mortality in Mexico is currently
174 driven primarily by cold [50] and that under climate change, temperature-related mortality will fall
175 in Mexico as the benefits from reduced cold outweigh the harms from increased heat [6]. Our results
176 present a more complicated picture: we find—consistent with prior literature—that temperature-
177 related mortality as a whole will fall in Mexico under climate change, but when taking age-specific
178 effects into account, we project that this will happen at the expense of younger individuals.

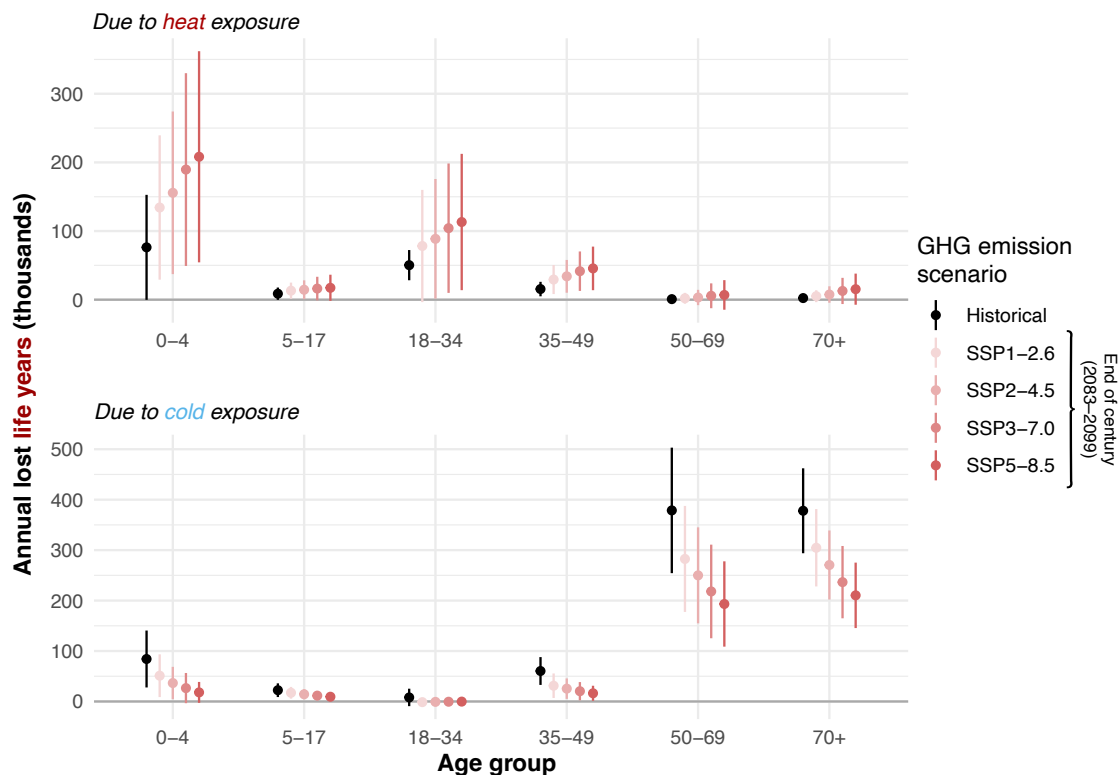


Figure 4: Historical and projected annual lost life years due to heat (top panel) and cold (bottom panel) exposure by age group

This figure mirrors Figure 3, but with the outcome as lost life years, rather than deaths. Potential remaining life years are taken from the UN World Population Prospects 2022, and are aggregated to time-invariant age group values by taking a population-weighted average across single age bins and years. The figure depicts the annual number of lost life years attributed to heat and cold exposure in Mexico historically and under wet-bulb temperatures prevailing at the end of the century in four greenhouse gas emission scenarios. The top panel indicates values for heat exposure, whereas the bottom panel indicates values for cold exposure. Whiskers above and below each estimate depict 95% confidence intervals net of both econometric and climate uncertainty.

179 4 Discussion

180 The unique combination of elements in this study—station-level wet-bulb temperature estimates,
 181 granular mortality data from across the entire age distribution in a country with a wide diversity
 182 of climatic conditions, a statistical method that captures age-specific heterogeneity in tempera-

183 ture vulnerability, and high-resolution projections of humid heat—deepens our understanding of
184 multiple aspects of the impact of temperature on mortality. By focusing on granular, age-specific
185 temperature-mortality impacts, our study contributes to the existing literature that has usually fo-
186 cused on mortality irrespective of age [1, 8, 52], across broader age groups [6, 42], or on the elderly
187 alone [12, 13]. In particular, in our setting, we find that while individuals 35 and older suffer the
188 vast majority of the cold-related mortality burden, those younger than 35 suffer the majority of
189 the heat-related mortality burden. In addition, we identify a source of climate-driven inequality
190 that has not been identified in previous studies: across all future emissions scenarios, we find that
191 climate change causes the temperature-related mortality burden to shift away from the elderly to-
192 wards the young. Given that temperature-related mortality is projected to be the largest single
193 source of climate damages [53, 54], the disproportionate burden of this impact on the young is likely
194 an important source of future climate-driven inequality.

195 Prior research has discussed multiple reasons that older individuals are vulnerable to cold tem-
196 peratures. These reasons are physiological, behavioral, and social. First, the elderly exhibit lower
197 shivering temperature thresholds [55] and have significantly lower levels of brown adipose tissue
198 (key for non-shivering thermogenesis) [56]. Second, a relatively large proportion of elderly individ-
199 uals have pre-existing medical conditions or attendant respiratory illnesses that can be contributing
200 factors in cold-related mortality [57]. Third, elderly individuals are increasingly living alone, mak-
201 ing it more difficult for them to access public health resources during extreme weather events, and
202 they experience higher rates of loneliness, which is correlated with worse cardiovascular health [58].
203 Fourth, energy poverty—spending a large fraction of income on energy—can be particularly acute
204 for elderly individuals. Mexico has both a high rate of energy poverty and a high prevalence of
205 credit constraints that might prevent adoption of protective but energy-intensive home heating [59].
206 In this study, we indeed find that the elderly are, in terms of absolute mortality impacts, far more
207 vulnerable to cold than other age groups (Figure S1). We find that the vast majority of cold-related
208 mortality is concentrated in those 50 and older, as shown in the top panels of Figure 2.

209 However, we find that young people are particularly vulnerable to heat: the majority of heat-
210 related deaths are concentrated in those under 35, and those under 35 are overrepresented in

211 heat-related deaths relative to their fraction of the population despite their far lower background
212 crude death rate (Figure S5). Our finding that children younger than five years old are especially
213 vulnerable to heat (Figure 1) is directionally consistent with some prior work, although we find par-
214 ticularly acute effects. Multiple potential mechanisms may contribute to this result. First, infants
215 have a higher body surface area to body weight ratio than adults, which means they gain heat more
216 rapidly and are more susceptible to overheating; infants also have a less developed thermoregulatory
217 system (exhibiting reduced sweating), which means they are not as efficient at regulating their body
218 temperature [60]. Second, very young children have less well-developed immune systems, making
219 them more vulnerable to climate-related infectious diseases including vector-borne diseases and
220 diarrheal diseases that might be especially affected by humid heat [61, 62]. Finally, both infants
221 and young children have less freedom of movement than adults and may not be able to express
222 their discomfort or distress as easily as adults, making it more difficult for caregivers—the primary
223 providers of child adaptation to heat exposure—to recognize and respond to their heat stress [63].

224 We also find that heat disproportionately affects those 18 to 34 years old. Younger adults
225 are more physiologically robust to heat, but multiple behavioral, social, and economic factors can
226 contribute to higher heat-related mortality among this age group [41]. Younger individuals are
227 exposed to ambient heat through sports and other recreational activities [41]. Households with
228 older household heads are more likely to have an air conditioner [64]. One important channel may
229 be occupational heat exposure: young adults are more likely than older adults to work in outdoor
230 occupations with minimal flexibility for precautionary action [65]. An analysis of death certificates
231 in Mexico shows that men of working age are more likely to have extreme weather events listed as
232 a cause of death [28]. Though we note that death certificates typically do not capture all deaths
233 due to extreme weather [66]. Relatedly, we find that individuals who live in regions with higher
234 income (itself correlated with the amount of weather-exposed occupations) are less sensitive to heat
235 (Figure S8). Occupational exposure is likely to be an important mechanism in other countries as
236 well given that Mexico is not out of the ordinary in terms of occupational exposure to heat. For
237 example, during our sample period 15% of the workforce in Mexico was employed in agriculture.
238 This is lower than the rate for other middle-income countries (30% in 2018) and all countries globally

239 (27% in 2018) [67]. If occupational heat exposure is indeed a driver of mortality among younger
240 individuals, this highlights the importance of occupational heat exposure standards for workers [68].

241 Our finding that young people in Mexico are especially vulnerable to heat may have global
242 implications because hotter and lower-income countries—which are expected to be the most ad-
243 versely impacted by climate change—have among the youngest populations in the world currently
244 and over the coming century [69]. Figure S12 shows the current global pattern of age and wet-bulb
245 temperature exposure. The map in the top panel breaks down countries by their most extreme
246 wet-bulb temperatures and fraction of population younger than 35 years of age [70]. The youngest
247 and hottest locations in the world are concentrated in Africa, Central America, the Middle East,
248 and portions of South and Southeast Asia. The bottom panel of Figure S12 situates Mexico in the
249 context of the rest of the world. Mexico is near the middle of the global distribution of countries by
250 share of population under 35, and its extreme wet-bulb temperatures are essentially only surpassed
251 by countries in Asia. The figure also shows that historical exposure to hot wet-bulb temperature
252 is positively correlated with the fraction of the population under 35. If our age-specific results in
253 this study hold for other countries around the world that are younger and hotter, then existing
254 estimates of temperature-related mortality impacts in these countries—which neither fully capture
255 age-specific heterogeneity in the temperature–mortality relationship nor account for the impact of
256 humid heat—may be incorrect. In past work, the lack of age-specific mortality data has been a
257 limiting factor in exploring the age-specific temperature-mortality relationship across a large num-
258 ber of countries [6, 52], which underscores the need for improvements in vital statistics systems,
259 especially in the places most vulnerable to climate change.

260 We conclude by highlighting a few important caveats and also point to potential areas of focus for
261 future work. Recent work has pioneered the use of both temperature and humidity for constrained
262 joint projections [38, 71, 72]. While regional and global climate models are our best tools for
263 assessments of future heat stress risk, the relatively coarse time resolution of most model output
264 limits the ability to project extreme values. The NEX-GDDP dataset used in this study reports
265 variables at a daily resolution, like many other climate models. Given the misalignment of the
266 diurnal cycles of temperature and humidity, using available daily mean values to calculate heat

267 stress metrics such as wet-bulb temperature limits the accuracy of daily mean projections and is
268 virtually impossible for daily maximum projections. These data challenges relating to the sub-daily
269 fluctuations in individual variables are even more pronounced for heat stress metrics such as wet-
270 bulb globe temperature (WBGT) that incorporate additional variables relevant to the physiology
271 of heat stress (e.g., solar insolation and wind speed) [73]. These limitations underpin efforts to
272 increase the temporal resolution of model data output available to end users in order to better
273 represent the most extreme heat stress conditions of the future.

274 Our projections assume that our estimated temperature–mortality relationships will remain
275 unchanged under future warming. There are opposing reasons why the exposure–response functions
276 to wet-bulb temperature may become either more or less severe in the future. Research on the U.S.
277 shows that mortality vulnerability to non-optimal dry-bulb temperatures has decreased historically
278 [74, 75]. Recent work has shown that locations with different long-run climates show different
279 patterns of consumption responses to weather shocks [76]. Figure S8 shows that a similar pattern
280 holds for mortality in Mexico. However, as wet-bulb temperatures approach uncompensable levels
281 with significantly greater frequency [34, 51]—exposures of this degree are almost nonexistent in the
282 historical record—we may learn that mortality associated with a given level of humid heat exposure
283 is worse than existing estimates. Furthermore, our projections hold socioeconomic conditions fixed.
284 Recently published subnational population projections for Mexico would allow future work to relax
285 this assumption [77]. Such projections could yield higher estimates of mortality if population
286 is trending younger in areas that are warming, or such projections could yield lower mortality
287 estimates if the population is becoming older over time. Further estimation of the effect of income
288 and occupational exposure could also enrich these projections and help shed light on the role of
289 adaptation in mediating temperature-related mortality. We leave the exploration of these questions
290 to future work.

291 Finally, our conclusions further underscore the importance of ethical choices around monetizing
292 the cost of premature deaths. We find that climate change is expected to shift the mortality burden
293 away from older individuals (more impacted by cold) to younger individuals (more impacted by
294 heat). Thus, the choice of whether to value life years—where premature deaths among younger

295 individuals are considered more costly than premature deaths among old individuals—or to value all
296 premature deaths the same, becomes especially important. The U.S. tends to value all premature
297 deaths the same in its benefit-cost analysis [78] whereas U.K. guidance suggests that analysts can
298 value either lives or life years [79]. Although we do not take a stance on this difficult ethical choice,
299 our findings further emphasize the importance of this debate for evaluations of the impact of climate
300 change, given that we are finding that climate change is expected to shift the temperature-related
301 mortality burden toward the young.

302 **5 Acknowledgements**

303 **5.1 Funding**

304 R.H. acknowledges the National Oceanic and Atmospheric Administration’s Climate Adaptation
305 Partnerships Program, grant NA21OAR4310313, which helped support this research. A.S. acknowl-
306 edges support from NSF Grant AGS-1758603.

307 **5.2 Author Contributions**

308 Conceptualization: AS, AW, CI, CT, JS, PK, RDB

309 Data curation: AW, CI, RDB, RH

310 Formal analysis: AW, CI, JS, RDB, RH

311 Methodology: AS, AW, CI, CT, CR, JS, RDB, RH

312 Project administration: AW, JS, RDB, RH

313 Supervision: AS, AW, JS, RDB, RH, PK

314 Visualization: AW, JS, RDB

315 Writing - original draft: AW, CI, JS, RDB

316 Writing - review & editing: AS, AW, CI, CT, CR, RH, PK, RDB, TC, JS

317 5.3 Competing Interests

318 All authors declare no competing interests.

319 5.4 Data and Materials Availability

320 All data needed to evaluate the conclusions in the paper are present in the paper and/or the
321 Supplementary Materials. A complete replication package can be found here.

322 References

- 323 1. Gasparrini, A. *et al.* Mortality risk attributable to high and low ambient temperature: a
324 multicountry observational study. en. *The Lancet* **386**, 369–375. ISSN: 01406736. [https://](https://linkinghub.elsevier.com/retrieve/pii/S0140673614621140)
325 linkinghub.elsevier.com/retrieve/pii/S0140673614621140 (2021) (July 2015).
- 326 2. Mitchell, D. *et al.* Attributing human mortality during extreme heat waves to anthropogenic
327 climate change. en. *Environmental Research Letters* **11**. Publisher: IOP Publishing, 074006.
328 ISSN: 1748-9326. <https://doi.org/10.1088%2F1748-9326%2F11%2F7%2F074006> (2020) (July
329 2016).
- 330 3. Vicedo-Cabrera, A. M. *et al.* The burden of heat-related mortality attributable to recent
331 human-induced climate change. en. *Nature Climate Change* **11**, 492–500. ISSN: 1758-678X,
332 1758-6798. <http://www.nature.com/articles/s41558-021-01058-x> (2021) (June 2021).
- 333 4. Bressler, R. D. The mortality cost of carbon. en. *Nature Communications* **12**, 4467. ISSN:
334 2041-1723. <https://www.nature.com/articles/s41467-021-24487-w> (2021) (July 2021).
- 335 5. Bressler, R. D., Moore, F. C., Rennert, K. & Anthoff, D. Estimates of country level temperature-
336 related mortality damage functions. en. *Scientific Reports* **11**, 20282. ISSN: 2045-2322. [https:](https://www.nature.com/articles/s41598-021-99156-5)
337 [//www.nature.com/articles/s41598-021-99156-5](https://www.nature.com/articles/s41598-021-99156-5) (2021) (Dec. 2021).
- 338 6. Carleton, T. *et al.* Valuing the global mortality consequences of climate change accounting for
339 adaptation costs and benefits. en. *The Quarterly Journal of Economics*, 69 (2022).

- 340 7. Chen, K. *et al.* Impact of climate change on heat-related mortality in Jiangsu Province, China.
341 en. *Environmental Pollution* **224**, 317–325. ISSN: 0269-7491. <http://www.sciencedirect.com/science/article/pii/S0269749116319303> (2020) (May 2017).
- 343 8. Cromar, K. R. *et al.* Global Health Impacts for Economic Models of Climate Change: A
344 Systematic Review and Meta-Analysis. eng. *Annals of the American Thoracic Society* **19**,
345 1203–1212. ISSN: 2325-6621 (July 2022).
- 346 9. Deschênes, O. & Greenstone, M. Climate Change, Mortality, and Adaptation: Evidence from
347 Annual Fluctuations in Weather in the US. *American Economic Journal: Applied Economics*
348 **3**, 152–185. ISSN: 1945-7782. <https://www.jstor.org/stable/41288654> (2018) (2011).
- 349 10. Gasparrini, A. *et al.* Projections of temperature-related excess mortality under climate change
350 scenarios. en. *The Lancet Planetary Health* **1**, e360–e367. ISSN: 25425196. <https://linkinghub.elsevier.com/retrieve/pii/S2542519617301560> (2019) (Dec. 2017).
- 352 11. Hajat, S., Vardoulakis, S., Heaviside, C. & Eggen, B. Climate change effects on human health:
353 projections of temperature-related mortality for the UK during the 2020s, 2050s and 2080s.
354 en. *J Epidemiol Community Health* **68**, 641–648. ISSN: 0143-005X, 1470-2738. <https://jech.bmj.com/content/68/7/641> (2020) (July 2014).
- 356 12. Hales, S. *et al.* *Quantitative risk assessment of the effects of climate change on selected causes*
357 *of death, 2030s and 2050s* en. OCLC: 897764432. ISBN: 978-92-4-150769-1. http://apps.who.int/iris/bitstream/10665/134014/1/9789241507691_eng.pdf (2019) (2014).
- 359 13. Honda, Y. *et al.* Heat-related mortality risk model for climate change impact projection.
360 en. *Environmental Health and Preventive Medicine* **19**, 56–63. ISSN: 1347-4715. <https://environhealthprevmed.biomedcentral.com/articles/10.1007/s12199-013-0354-6>
361 (2019) (Jan. 2014).
- 363 14. Houser, T. *et al.* *Economic Risks of Climate Change: An American Prospectus* en. Google-
364 Books-ID: 0QTSBgAAQBAJ. ISBN: 978-0-231-53955-5 (Columbia University Press, Aug. 2015).

- 365 15. Kingsley Samantha L., Eliot Melissa N., Gold Julia, Vanderslice Robert R. & Wellenius Gre-
366 gory A. Current and Projected Heat-Related Morbidity and Mortality in Rhode Island. *En-*
367 *vironmental Health Perspectives* **124**, 460–467. [https://ehp.niehs.nih.gov/doi/full/10.](https://ehp.niehs.nih.gov/doi/full/10.1289/ehp.1408826)
368 [1289/ehp.1408826](https://ehp.niehs.nih.gov/doi/full/10.1289/ehp.1408826) (2020) (2016).
- 369 16. Knowlton, K. *et al.* Projecting Heat-Related Mortality Impacts Under a Changing Climate in
370 the New York City Region. en. *American Journal of Public Health* **97**, 2028–2034. ISSN: 0090-
371 0036, 1541-0048. <http://ajph.aphapublications.org/doi/10.2105/AJPH.2006.102947>
372 (2020) (Nov. 2007).
- 373 17. Kim, D.-W., Deo, R. C., Chung, J.-H. & Lee, J.-S. Projection of heat wave mortality related
374 to climate change in Korea. en. *Natural Hazards* **80**, 623–637. ISSN: 0921-030X, 1573-0840.
375 <http://link.springer.com/10.1007/s11069-015-1987-0> (2020) (Jan. 2016).
- 376 18. Lee, J. Y. & Kim, H. Projection of future temperature-related mortality due to climate and
377 demographic changes. en. *Environment International* **94**, 489–494. ISSN: 0160-4120. [http://](http://www.sciencedirect.com/science/article/pii/S0160412016302252)
378 www.sciencedirect.com/science/article/pii/S0160412016302252 (2020) (Sept.
379 2016).
- 380 19. Li, T., Horton, R. M. & Kinney, P. L. Projections of seasonal patterns in temperature- related
381 deaths for Manhattan, New York. en. *Nature Climate Change* **3**, 717–721. ISSN: 1758-6798.
382 <https://www.nature.com/articles/nclimate1902> (2020) (Aug. 2013).
- 383 20. Marsha, A., Sain, S. R., Heaton, M. J., Monaghan, A. J. & Wilhelmi, O. Influences of cli-
384 matic and population changes on heat-related mortality in Houston, Texas, USA. en. *Climatic*
385 *Change* **146**, 471–485. ISSN: 0165-0009, 1573-1480. [http://link.springer.com/10.1007/](http://link.springer.com/10.1007/s10584-016-1775-1)
386 [s10584-016-1775-1](http://link.springer.com/10.1007/s10584-016-1775-1) (2020) (Feb. 2018).
- 387 21. Martínez-Solanas, È. *et al.* Projections of temperature-attributable mortality in Europe: a time
388 series analysis of 147 contiguous regions in 16 countries. eng. *The Lancet. Planetary Health* **5**,
389 e446–e454. ISSN: 2542-5196 (July 2021).

- 390 22. Peng Roger D. *et al.* Toward a Quantitative Estimate of Future Heat Wave Mortality under
391 Global Climate Change. *Environmental Health Perspectives* **119**, 701–706. <https://ehp.niehs.nih.gov/doi/full/10.1289/ehp.1002430> (2020) (May 2011).
- 393 23. Petkova, E., Horton, R., Bader, D. & Kinney, P. Projected Heat-Related Mortality in the U.S.
394 Urban Northeast. en. *International Journal of Environmental Research and Public Health* **10**,
395 6734–6747. ISSN: 1660-4601. <http://www.mdpi.com/1660-4601/10/12/6734> (2020) (Dec.
396 2013).
- 397 24. Schwartz, J. D. *et al.* Projections of temperature-attributable premature deaths in 209 U.S.
398 cities using a cluster-based Poisson approach. en. *Environmental Health* **14**, 85. ISSN: 1476-
399 069X. <http://ehjournal.biomedcentral.com/articles/10.1186/s12940-015-0071-2>
400 (2020) (Dec. 2015).
- 401 25. Shindell, D. *et al.* The Effects of Heat Exposure on Human Mortality Throughout the United
402 States. en. *GeoHealth* **4**. ISSN: 2471-1403, 2471-1403. <https://onlinelibrary.wiley.com/doi/10.1029/2019GH000234> (2021) (2020).
- 404 26. Yang, J. *et al.* Projecting heat-related excess mortality under climate change scenarios in
405 China. en. *Nature Communications* **12**, 1039. ISSN: 2041-1723. <http://www.nature.com/articles/s41467-021-21305-1> (2021) (Dec. 2021).
- 407 27. Zhang, B., Li, G., Ma, Y. & Pan, X. Projection of temperature-related mortality due to
408 cardiovascular disease in beijing under different climate change, population, and adaptation
409 scenarios. en. *Environmental Research* **162**, 152–159. ISSN: 00139351. <https://linkinghub.elsevier.com/retrieve/pii/S001393511731770X> (2020) (2018).
- 411 28. Jáuregui-Díaz, J. A., Sánchez, M. d. J. Á. & Cabañas, R. T. Cambios en la Mortalidad por
412 Eventos Climáticos Extremos en México entre el 2000 y 2015. *Revista de Estudios Latinoamericanos sobre Reducción del Riesgo de Desastres REDER* **4**, 80–94 (2020).
- 414 29. Li, T. *et al.* Aging Will Amplify the Heat-related Mortality Risk under a Changing Climate:
415 Projection for the Elderly in Beijing, China. en. *Scientific Reports* **6**, 28161. ISSN: 2045-2322.
416 <http://www.nature.com/articles/srep28161> (2020) (June 2016).

- 417 30. Mora, C. *et al.* Global risk of deadly heat. en. *Nature Climate Change* **7**, 501–506. ISSN:
418 1758-6798. <https://www.nature.com/articles/nclimate3322> (2019) (July 2017).
- 419 31. Armstrong, B. *et al.* The role of humidity in associations of high temperature with mortality:
420 a multicountry, multicity study. *Environmental health perspectives* **127**, 097007 (2019).
- 421 32. Raymond, C., Matthews, T. & Horton, R. M. The emergence of heat and humidity too severe
422 for human tolerance. *Science Advances* **6**, eaaw1838 (2020).
- 423 33. Sherwood, S. C. & Huber, M. An adaptability limit to climate change due to heat stress.
424 *Proceedings of the National Academy of Sciences* **107**, 9552–9555 (2010).
- 425 34. Vecellio, D. J., Wolf, S. T., Cottle, R. M. & Kenney, W. L. Evaluating the 35°C wet-bulb
426 temperature adaptability threshold for young, healthy subjects (PSU HEAT Project). *Journal*
427 *of Applied Physiology* **132**. Publisher: American Physiological Society, 340–345. ISSN: 8750-
428 7587. <https://journals.physiology.org/doi/full/10.1152/jappphysiol.00738.2021>
429 (2023) (Feb. 2022).
- 430 35. Vanos, J. *et al.* A physiological approach for assessing human survivability and liveability to
431 heat in a changing climate. en. *Nature Communications* **14**, 7653. ISSN: 2041-1723. [https://](https://www.nature.com/articles/s41467-023-43121-5)
432 www.nature.com/articles/s41467-023-43121-5 (2024) (Nov. 2023).
- 433 36. Baldwin, J. W. *et al.* Humidity’s Role in Heat-Related Health Outcomes: A Heated Debate.
434 en. *Environmental Health Perspectives* **131**, 055001. ISSN: 0091-6765, 1552-9924. [https://](https://ehp.niehs.nih.gov/doi/10.1289/EHP11807)
435 ehp.niehs.nih.gov/doi/10.1289/EHP11807 (2023) (May 2023).
- 436 37. Havenith, G. & Fiala, D. Thermal indices and thermophysiological modeling for heat stress.
437 *Comprehensive Physiology* **6**. Publisher: Wiley Online Library, 255–302 (2011).
- 438 38. Buzan, J. R. & Huber, M. Moist Heat Stress on a Hotter Earth. en. *Annual Review of Earth*
439 *and Planetary Sciences* **48**, 623–655 (2020).
- 440 39. Parsons, K. *Human thermal environments: the effects of hot, moderate, and cold environments*
441 *on human health, comfort, and performance* (CRC press, 2014).

- 442 40. Steadman, R. G. The assessment of sultriness. Part I: A temperature-humidity index based
443 on human physiology and clothing science. *Journal of Applied Meteorology and Climatology*
444 **18**, 861–873 (1979).
- 445 41. Ebi, K. L. *et al.* Hot weather and heat extremes: health risks. *Lancet* **398**, 698–708 (2021).
- 446 42. Gallo, E. *et al.* Heat-related mortality in Europe during 2023 and the role of adaptation in
447 protecting health. en. *Nature Medicine* (2024).
- 448 43. Davies-Jones, R. An Efficient and Accurate Method for Computing the Wet-Bulb Temperature
449 along Pseudoadiabats. en. *Monthly Weather Review* **136**, 2764–2785. ISSN: 1520-0493, 0027-
450 0644. <http://journals.ametsoc.org/doi/10.1175/2007MWR2224.1> (2023) (July 2008).
- 451 44. Schwartz, J. Harvesting and long term exposure effects in the relation between air pollution
452 and mortality. *American Journal of Epidemiology* **151**, 440–448 (2000).
- 453 45. Thrasher, B., Maurer, E. P., McKellar, C. & Duffy, P. B. Bias correcting climate model simu-
454 lated daily temperature extremes with quantile mapping. *Hydrology and Earth System Sciences*
455 **16**, 3309–3314 (2012).
- 456 46. Riahi, K. *et al.* The Shared Socioeconomic Pathways and their energy, land use, and greenhouse
457 gas emissions implications: An overview. *Global environmental change* **42**, 153–168 (2017).
- 458 47. Dunn, R. J. H., Willett, K. M., Parker, D. E. & Mitchell, L. Expanding HadISD: quality-
459 controlled, sub-daily station data from 1931. *Geoscientific Instrumentation, Methods and Data*
460 *Systems* **5**, 473–491. <https://gi.copernicus.org/articles/5/473/2016/> (2016).
- 461 48. Muñoz-Sabater, J. *et al.* ERA5-Land: a state-of-the-art global reanalysis dataset for land
462 applications. *Earth System Science Data* **13**, 4349–4383. [https://essd.copernicus.org/](https://essd.copernicus.org/articles/13/4349/2021/)
463 [articles/13/4349/2021/](https://essd.copernicus.org/articles/13/4349/2021/) (2021).
- 464 49. Raymond, C. *et al.* Regional and elevational patterns of extreme heat stress change in the US.
465 *Environmental Research Letters* **17**, 064046 (2022).
- 466 50. Cohen, F. & Dechezleprêtre, A. Mortality, temperature, and public health provision: evidence
467 from Mexico. *American Economic Journal: Economic Policy* **14**, 161–192 (2022).

- 468 51. Powis, C. M. *et al.* Observational and model evidence together support wide-spread exposure
469 to noncompensable heat under continued global warming. *Science Advances* **9**. Publisher:
470 American Association for the Advancement of Science, eadg9297. <https://www.science.org/doi/10.1126/sciadv.adg9297> (2023) (Sept. 2023).
471
- 472 52. Wu, Y. *et al.* Global, regional, and national burden of mortality associated with short-term
473 temperature variability from 2000–19: a three-stage modelling study. *The Lancet Planetary*
474 *Health* **6**, e410–e421. ISSN: 2542-5196. <https://www.sciencedirect.com/science/article/pii/S2542519622000730> (2023) (May 2022).
475
- 476 53. EPA. *Supplementary Material for the Regulatory Impact Analysis for the Supplemental Pro-*
477 *posed Rulemaking, “Standards of Performance for New, Reconstructed, and Modified Sources*
478 *and Emissions Guidelines for Existing Sources: Oil and Natural Gas Sector Climate Review”*
479 Sept. 2022. <https://t.co/Q11VBWDGmL>.
- 480 54. Rennert, K. *et al.* Comprehensive evidence implies a higher social cost of CO₂. en. *Nature*
481 **610**. Number: 7933 Publisher: Nature Publishing Group, 687–692. ISSN: 1476-4687. <https://www.nature.com/articles/s41586-022-05224-9> (2023) (Oct. 2022).
482
- 483 55. Vassilieff, N., Rosencher, N., Sessler, D. I. & Conseiller, C. Shivering threshold during spinal
484 anesthesia is reduced in elderly patients. *The Journal of the American Society of Anesthesiol-*
485 *ogists* **83**, 1162–1166 (1995).
- 486 56. Saely, C. H., Geiger, K. & Drexel, H. Brown versus white adipose tissue: a mini-review. *Geron-*
487 *tology* **58**, 15–23 (2011).
- 488 57. Zanobetti, A., O’Neill, M. S., Gronlund, C. J. & Schwartz, J. D. Susceptibility to mortality in
489 weather extremes: effect modification by personal and small area characteristics in a multi-city
490 case-only analysis. *Epidemiology (Cambridge, Mass.)* **24**, 809 (2013).
- 491 58. Leigh-Hunt, N. *et al.* An overview of systematic reviews on the public health consequences of
492 social isolation and loneliness. *Public health* **152**, 157–171 (2017).

- 493 59. Soriano-Hernandez, P., Mejia-Montero, A. & van der Horst, D. Characterisation of energy
494 poverty in Mexico using energy justice and econophysics. *Energy for Sustainable Development*
495 **71**, 200–211 (2022).
- 496 60. Falk, B. & Dotan, R. Children’s thermoregulation during exercise in the heat—a revisit. *Ap-
497 plied Physiology, Nutrition, and Metabolism* **33**, 420–427 (2008).
- 498 61. Xu, Z. *et al.* Impact of ambient temperature on children’s health: A systematic review. en.
499 *Environmental Research* **117**, 120–131. ISSN: 00139351. [https://linkinghub.elsevier.
500 com/retrieve/pii/S0013935112001983](https://linkinghub.elsevier.com/retrieve/pii/S0013935112001983) (2022) (Aug. 2012).
- 501 62. Brown, J. J., Pascual, M., Wimberly, M. C., Johnson, L. R. & Murdock, C. C. Humidity—The
502 overlooked variable in the thermal biology of mosquito-borne disease. *Ecology Letters* (2023).
- 503 63. Graff Zivin, J. & Shrader, J. Temperature extremes, health, and human capital. *The Future
504 of Children*, 31–50 (2016).
- 505 64. Pavanello, F. *et al.* Air-conditioning and the adaptation cooling deficit in emerging economies.
506 *Nature communications* **12**, 6460 (2021).
- 507 65. Kjellström, T., Maitre, N., Saget, C., Otto, M. & Karimova, T. *Working on a warmer planet:
508 The impact of heat stress on labour productivity and decent work* (ILO, 2019).
- 509 66. Green, H. K. *et al.* Challenges with disaster mortality data and measuring progress towards
510 the implementation of the Sendai framework. *International Journal of Disaster Risk Science*
511 **10**, 449–461 (2019).
- 512 67. International Labour Organization. *ILO modelled estimates database* Accessed February 07,
513 2024. 2024. <https://ilostat.ilo.org/data/>.
- 514 68. OSHA. Heat injury and illness prevention in outdoor and indoor work settings. *Federal Register*
515 (2024).
- 516 69. Gaigbe-Togbe, V., Bassarsky, L., Gu, D., Spoorenberg, T. & Zeifman, L. World population
517 prospects 2022. *Department of Economic and Social Affairs, Population Division: New York,
518 NY, USA* (2022).

- 519 70. For Economic, U. N. D. & Affairs, S. *World Population Prospects 2022: Summary of results*
520 (UN, 2023).
- 521 71. Fischer, E. M. & Knutti, R. Robust projections of combined humidity and temperature ex-
522 tremes. en. *Nature Climate Change* **3**, 126–130. ISSN: 1758-678X, 1758-6798. <https://www.nature.com/articles/nclimate1682> (2023) (Feb. 2013).
523
- 524 72. Yuan, J., Stein, M. L. & Kopp, R. E. The evolving distribution of relative humidity conditional
525 upon daily maximum temperature in a warming climate. *Journal of Geophysical Research:*
526 *Atmospheres* **125**, e2019JD032100 (2020).
- 527 73. Buzan, J. R., Oleson, K. & Huber, M. Implementation and comparison of a suite of heat stress
528 metrics within the Community Land Model version 4.5. en. *Geoscientific Model Development*
529 **8**, 151–170. ISSN: 1991-9603. <https://gmd.copernicus.org/articles/8/151/2015/> (2024)
530 (Feb. 2015).
- 531 74. Barreca, A., Clay, K., Deschenes, O., Greenstone, M. & Shapiro, J. S. Adapting to climate
532 change: The remarkable decline in the US temperature-mortality relationship over the twen-
533 tieth century. *Journal of Political Economy* **124**, 105–159 (2016).
- 534 75. Shrader, J., Bakkensen, L. & Lemoine, D. Fatal Errors: The Mortality Value of Accurate
535 Weather Forecasts. *IZA Discussion Paper* **16253**, 1–41. https://papers.ssrn.com/sol3/papers.cfm?abstract_id=4490162 (2023).
536
- 537 76. Lai, W., Li, S., Liu, Y. & Barwick, P. J. Adaptation mitigates the negative effect of temperature
538 shocks on household consumption. *Nature Human Behaviour* **6**, 837–846 (2022).
- 539 77. Regules García, R., Gómez-Ugarte, A. C., Zoraghein, H. & Jiang, L. Sub-National Population
540 Projections for Mexico Under the Shared Socioeconomic Pathways (SSPs) in the Context of
541 Climate Change. *Population Research and Policy Review* **43**, 44. ISSN: 1573-7829. (2024) (June
542 2024).
- 543 78. OMB. *Circular A-4* en. Nov. 2023. [https://www.whitehouse.gov/wp-content/uploads/](https://www.whitehouse.gov/wp-content/uploads/2023/11/CircularA-4.pdf)
544 [2023/11/CircularA-4.pdf](https://www.whitehouse.gov/wp-content/uploads/2023/11/CircularA-4.pdf).

- 545 79. HM Treasury. *The Green Book: Appraisal and Evaluation in Central Government* en. [https://www.gov.uk/government/publications/the-green-book-appraisal-and-evaluation-](https://www.gov.uk/government/publications/the-green-book-appraisal-and-evaluation-in-central-government)
546 [in-central-government](https://www.gov.uk/government/publications/the-green-book-appraisal-and-evaluation-in-central-government) (2023) (HM Treasury, 2022).
- 548 80. Lab, F. C. & for International Earth Science Information Network – CIESIN – Columbia
549 University, C. *High Resolution Settlement Layer (HRSL)* Source imagery for HRSL © 2016
550 DigitalGlobe. 2016.
- 551 81. Harrell, F. E. *Regression Modeling Strategies: With Applications to Linear Models, Logistic*
552 *and Ordinal Regression, and Survival Analysis* ISBN: 9783319194257. [http://dx.doi.org/](http://dx.doi.org/10.1007/978-3-319-19425-7)
553 [10.1007/978-3-319-19425-7](http://dx.doi.org/10.1007/978-3-319-19425-7) (Springer International Publishing, 2015).
- 554 82. Bergé, L. Efficient estimation of maximum likelihood models with multiple fixed-effects: the
555 R package FENmlm. *CREA Discussion Papers* (2018).
- 556 83. Dong, J., Bronniman, S., Hu, T., Liu, Y. & Peng, J. GSDM-WBT: Global station-based daily
557 maximum wet-bulb temperature data for 1981-2020. *Earth System Science Data* (2022).
- 558 84. Sims, K. *et al. LandScan Global 2022* <https://landscan.ornl.gov> (2023).

559 **A Supplementary Materials**

560 **A.1 Data**

561 **A.1.1 Mortality, population, and life expectancy data**

562 We collect mortality data from the Subsistema de Información Demográfica y Social of Mexico's
563 Instituto Nacional de Estadística y Geografía. This data contains records of all recorded mortality
564 events in Mexico since 1990. Our data period begins in 1998, when this mortality microdata first
565 began to carry information about the day and municipality of each mortality event. Our data period
566 ends in 2019, after which some death records are still preliminary and the COVID-19 pandemic
567 exerts a large influence on behavior and mortality. Between 1998 and 2019, we observe in this
568 data 13,426,931 deaths. The World Bank estimates that Mexico's all-cause crude mortality rate is
569 around 6 deaths per 1000 people per year. Relative to a population of around 110 million during this
570 period, this would imply total deaths of 14.5 million during our data period, giving us confidence
571 that these mortality records are relatively complete. Across the data, each recorded mortality
572 event also contains information on the cause of the individual's death as well as the individual's
573 sex, education level, occupation, place of residence, and age at death. We drop death records that
574 are missing information on the day of death, the individual's age at death, or the death location. We
575 also drop death records reporting deaths that occurred outside of Mexico. These dropped records
576 represent less than 0.92% of the data.

577 Data on administrative unit population, which is used to determine mortality rates and regres-
578 sion weights, is collected from IPUMS International, which consolidates and harmonizes census data
579 for Mexico. Our study uses data from the 1990, 2000, and 2010 Mexican censuses, as well as the
580 2015 Intercensal Survey. Population for each administrative unit is assumed to grow at a constant
581 rate between observations, and population growth between the 2010 Census and 2015 Intercensal
582 Survey is assumed to remain constant through the end of our data in 2019.

583 Across both mortality and population data, we account for 67 municipal boundary changes
584 occurring between 1998 and 2019 by assigning values reported for modified units to an aggregate
585 set of 2,402 municipal units that is stable across all years of our study. We also aggregate deaths

586 and population across age groups: age (1) less than 5, (2) at least 5 and less than 18, (3) at least
587 18 and less than 35, (4) at least 35 and less than 50, (5) at least 50 and less than 70, (6) at least
588 70.

589 In this study, we sometimes report values in terms of lost life years. Our estimates for the
590 age-dependent number of remaining life years at time of death for the average person in each age
591 group come from the United Nations 2022 World Population Prospects, with expected remaining
592 life years for an age group calculated as a weighted mean of the expected remaining life years of
593 cohorts in each age classification across all sample years (i.e., expected remaining life years of those
594 less than 5 is estimated as the expected remaining life years of age cohorts aged 0, 1, 2, 3, and 4
595 across every year from 1998 to 2019, weighted by the population size of each cohort). The resulting
596 scalars are not particularly sensitive to the aggregation procedure, as potential remaining life years
597 did not change markedly for any age group in Mexico during our data period. The scalars range
598 from 73.32 expected remaining life years for the under-5 age group to 9.91 expected remaining life
599 years for the 70+ age group.

600 **A.1.2 Weather data**

601 Our observational weather dataset is collected from the UK Met Office Hadley Centre’s Integrated
602 Surface Dataset, which consolidates observations from a global network of weather stations but per-
603 forms various quality control adjustments to ensure the consistency of observations over time. The
604 resulting dataset we use contains a set of weather metrics recorded at a sub-daily frequency (some
605 stations report weather at an hourly frequency, but many report at three- or six-hour intervals). A
606 map of the stations reporting data used in our analysis is shown in Figure S14.

607 Extreme wet-bulb temperature events at thresholds sufficiently high to impact human health
608 may be short in duration and tightly spatially constrained [32]. Accordingly, recent literature has
609 suggested that the spatial and temporal smoothing involved in the creation of reanalysis products
610 often leads to underestimations of the intensity of extreme humid heat events compared to observa-
611 tional datasets [32]. We find that current high-resolution reanalysis data (ERA5-Land) are unable
612 to capture humid heat extremes. This is a known limitation of reanalysis products, though recent

613 work has argued that reanalysis products may be suitable for studies exploring the relationship
614 between temperature and mortality. This is not the case when such studies consider humidity,
615 which varies more over space. Indeed, many of the most extreme humid heat events arise from
616 short-lived intrusions of moist air above very warm seas into coastal cities on very hot days, a point
617 emphasized in [32].

618 We first use the method described in [43] to approximate wet-bulb temperature from dry-
619 bulb temperature, surface pressure, and dew point temperature at each station location. As our
620 method requires matching station temperature records to administrative units, we then perform
621 an adjustment to fill missing hourly dry-bulb and wet-bulb temperature observations by leveraging
622 distributional information from nearby non-missing stations. To avoid filling missing data for
623 stations that report infrequently or for which we do not have a sufficiently diverse historical record,
624 we first drop from our data all stations that report fewer than 10,000 observations during the period
625 from 1990 to 2019 (roughly 3% of hours) as well as stations that do not report more than 1000
626 observations across at least 10 years. For each of the remaining stations, we then determine an
627 empirical cumulative distribution function for all non-missing observations. Next, if the data does
628 not contain an observation for a given station at a particular hour, we determine a likely quantile
629 for this observation using an inverse squared geodesic distance-weighted mean of all stations in
630 Mexico that are reporting values at that hour. We then fill the missing value using the temperature
631 at that quantile for that station. Said differently, if a station is missing data at a particular hour
632 and nearby non-missing temperatures are on average at their 90th percentile, we set the missing
633 value to the 90th percentile of the historical readings for that station. This method is deployed in
634 the dataset here.

635 We obtain daily mean dry-bulb and wet-bulb temperatures by calculating the average of the
636 daily minima and maxima of each metric at each station. We next determine the geodesic distance
637 between each station and the population-weighted centroid of each administrative unit and map
638 temperature observations to administrative units by taking the inverse squared distance-weighted
639 mean of each temperature metric for the five nearest stations (see Figure S14 for the locations of
640 stations used in the study). This method is similar to other papers studying temperature effects on

641 mortality using weather station data [74]. To determine the population-weighted centroid of each
 642 administrative unit, we use Meta’s High-Resolution Population Density Maps [80]. To ensure that
 643 we are using representative weather station data to estimate exposure, we omit from our analysis
 644 municipalities whose population center of mass is more than 50 kilometers from the nearest weather
 645 station. These municipalities represent 24.83% of Mexico’s population as of the date of the 2010
 646 Census.

647 Precipitation data is collected from the European Centre for Medium-range Weather Forecasting
 648 Reanalysis 5 - Land (ERA5-Land) dataset (and included as a control to avoid confounding effects).
 649 Using Google Earth Engine, a daily total precipitation measure is calculated by taking a sum over
 650 the hourly values across each day at each grid cell and then taking a spatial average over each
 651 administrative unit, weighting by a gridded estimate of the time-varying distribution of population
 652 (Gridded Population of the World v4, revision 11).

653 A.2 Statistical model

654 Estimates of the effect of temperature on mortality come from fitting a mortality response function
 655 following [1]. The outcome variables—daily, location-specific mortality rates for each age group—
 656 are modeled as dynamic functions of temperature and precipitation, with additional controls for
 657 location-specific, time-varying, and seasonal confounders. Formally,

$$\begin{aligned}
 y_{ait} = & f_a(x_{it}, \dots, x_{it-30}; \mathbf{B}_a) + g_a(p_{it}, \dots, p_{it-30}; \mathbf{\Gamma}_a) \\
 & + \rho_{at} + \delta_{ai} \times \text{year}_t + \theta_{as} \times h(\text{doy}_t; \xi_a) + \varepsilon_{ait}
 \end{aligned}
 \tag{S-1}$$

658 where y_{ait} is the mortality rate (deaths per person) in municipality i on date t and age group
 659 $a \in \{< 5, 5-17, 18-34, 35-49, 50-69, > 70\}$. Separate models are fit for each age group.

660 The main right-hand-side variable is daily average temperature—either dry-bulb or wet-bulb
 661 depending on the specification—generically denoted x_{it} in the above equation. The relationship
 662 between temperature and mortality is allowed to be nonlinear and dynamic, as captured by the func-
 663 tion $f_a(x_{it}, \dots, x_{it-30}; \mathbf{B}_a)$, with \mathbf{B}_a denoting the matrix of unknown coefficients to be estimated.

664 This function transforms temperature observations along two dimensions. In the temperature di-
665 mension, the function is a natural cubic spline over daily temperature with knots at the 10th, 50th,
666 and 90th percentiles [81]. (For dry-bulb temperature, these knots are at approximately 14.92, 20.63,
667 and 27.51°C; for wet-bulb temperature, they are at approximately 9.14, 15.37, and 22.80°C.) Across
668 22 days of distributed lags, the function is a b-spline with knots spaced equally, in log terms, across
669 the lag period (at roughly 1, 3, and 8 days). Putting these elements together, fitting the model
670 generates estimates of the effect of temperature on mortality at each point across the distribution
671 of temperatures and for each of 22 days starting with with the initial day of the temperature real-
672 ization. From these estimates, we calculate and report the 21-day cumulative effect of temperature
673 on mortality, as depicted in Figure 1.

674 The other elements of the estimating equation are controls. Daily total precipitation, p_{it} is
675 included in a similar way to temperature, with the cumulative effect estimated using a b-spline
676 distributed lag. The effect of precipitation is modeled flexibly using 0th-order splines (i.e., bins)
677 for precipitation below the 80th percentile (roughly zero precipitation), between the 80th and 90th
678 percentiles, between the 90th and 95th percentiles, between the 95th and 98th percentiles, between
679 the 98th and 99.5th percentiles, and above the 99.5th percentile (the levels of these breaks are
680 approximately 5.31, 10.5, 15.6, 23.7, and 45.3 mm/day). Other confounders are accounted for using
681 fixed effects, in some cases interacted with continuous controls. These controls are: date of sample
682 fixed effects, ρ_{at} , to account for national temporal patterns, holidays, day-of-week effects, and other
683 time-series confounders; a municipality-by-year fixed effect, $\delta_{ai} \times \text{year}_t$, to account for location-
684 specific fixed factors such as topography, governance, and differences in access to healthcare or
685 mortality reporting as well as secular changes in mortality rates and climate; and a state-level fixed
686 effect, θ_{as} , interacted with a six-knot natural cubic spline over day-of-year, $h(\text{doy}_t; \xi_a)$, to account
687 for state-level seasonal patterns. The term ϵ_{ait} is the remaining error term which we assume to be
688 uncorrelated with daily temperature.

689 The regression is weighted by the daily municipality population (linearly interpolated from an-
690 nual population counts). Standard errors are clustered at the state level to account for spatial
691 autocovariances at the subnational level while maintaining robustness to arbitrary temporal corre-

692 lation patterns ($N = 32$).

693 Throughout, such as when we distinguish deaths from heat from those from cold or when we
694 report the total number of temperature-related deaths, we are identifying these values relative
695 to an age group-specific optimal temperature, or minimum mortality temperature (MMT). While
696 semantically the MMT is simply the temperature at which mortality is minimized, the flexible
697 functional form we use to determine the relationship between temperature and mortality leads to
698 a corner solution for the global MMT for some age groups. To prevent this, we instead define the
699 MMT conditionally as the temperature between the 1st and 99th percentiles of age group-specific
700 temperature exposure at which mortality is minimized [1]. As we discuss in the main body text,
701 MMT varies considerably by age, generally rising throughout the lifespan.

702 Models are fit using R software version 4.2.2 and the `fixest` package version 0.11.2 [82].

703 **A.3 Projections**

704 In addition to identifying historical relationships between wet-bulb temperature and mortality, we
705 make projections of the impact of climate change on these relationships through the end of the
706 century. The projections focus on the effect of changes in dry and moist heat, holding all other
707 aspects of the system fixed. To make temperature-related mortality projections, we apply the age-
708 specific exposure-response functions estimated from our statistical model to the future temperature
709 projections described above, and assume that these functions will continue to hold in the future,
710 as in [10]. Thus, we hold the severity of the effect of wet- and dry-bulb temperature on mortality
711 and the demographic characteristics of the country fixed, then change the levels of experienced wet-
712 and dry-bulb temperatures. This method facilitates comparison between the effect of current and
713 future climates.

714 For the climate projections, and again motivated by the need to capture fine scale spatial vari-
715 ability in dry and humid heat, we select the NASA Earth exchange Global Daily Downscaled
716 Projections (NEX-GDDP) dataset, a product statistically downscaled from Coupled Model Inter-
717 comparison Project Phase 6 (CMIP6) General Circulation Models (GCMs), as the underlying data
718 for our projections. This downscaled product provides daily data at a spatial resolution of 0.25 de-

719 grees, significantly more fine than the underlying CMIP6 models which primarily have a resolution
720 of approximately 1 degree. In order to apply the statistical model to various future periods and
721 measure the potential changes in the differential impacts of humid and dry heat on human health,
722 the variables necessary for projections include daily mean dry-bulb temperature, daily mean spe-
723 cific humidity, daily mean pressure, and daily total precipitation. Because the NEX-GDDP dataset
724 does not supply daily mean pressure data, we use an elevation-based approximation at each point.
725 While this method ignores the wet-bulb temperature effects of temporal pressure fluctuations, the
726 resultant bias is no more than approximately 0.25°C [83]. Twenty six models are selected based on
727 their inclusion of these variables. We perform projections for one ensemble member using green-
728 house gas emission pathways from four Shared Socioeconomic Pathway (SSP) scenarios, namely
729 SSPs 1-2.6, 2-4.5, 3-7.0, and 5-8.5.

730 We then use percentile mapping to generate synthetic time series for each meteorological vari-
731 able (dry-bulb temperature and precipitation as downloaded directly from NEX-GDDP; wet-bulb
732 temperature calculated from NEX-GDDP data as described above) during an end-of-century pe-
733 riod. Within each model and SSP GHG emissions scenario, data from the historical and future
734 periods are binned into 1 percentile bins (e.g., 1^{st} percentile, 2^{nd} percentile, \dots , 99^{th} percentile).
735 The delta change for each variable in these percentiles is computed between the historical period
736 and future periods. These percentile-specific change factors are then applied to the corresponding
737 percentile days in the observational station data. This approach retains any seasonality and internal
738 variability recorded in the observational historical period, is flexible, and allows for the mean and
739 higher moments of the future distribution of temperatures to be different than what was observed
740 historically.

741 To ensure comparability between average annual outcomes in the past and in projections, we cal-
742 culate past average annual outcomes using only exposures from 1998–2014. This period represents
743 the overlap between our mortality data (1998–2019) and the historical period for NEX-GDDP
744 models (1950–2015). The mid-century (2043–2059) and end-of-century (2083–2099) periods are
745 defined to be the same length as this past period, 17 years. Throughout, we use the term “histor-
746 ical” to refer to the period 1998–2014; when discussing the data period over which we resolve our

⁷⁴⁷ exposure–response functions (1998–2019), we use the term “sample period.”

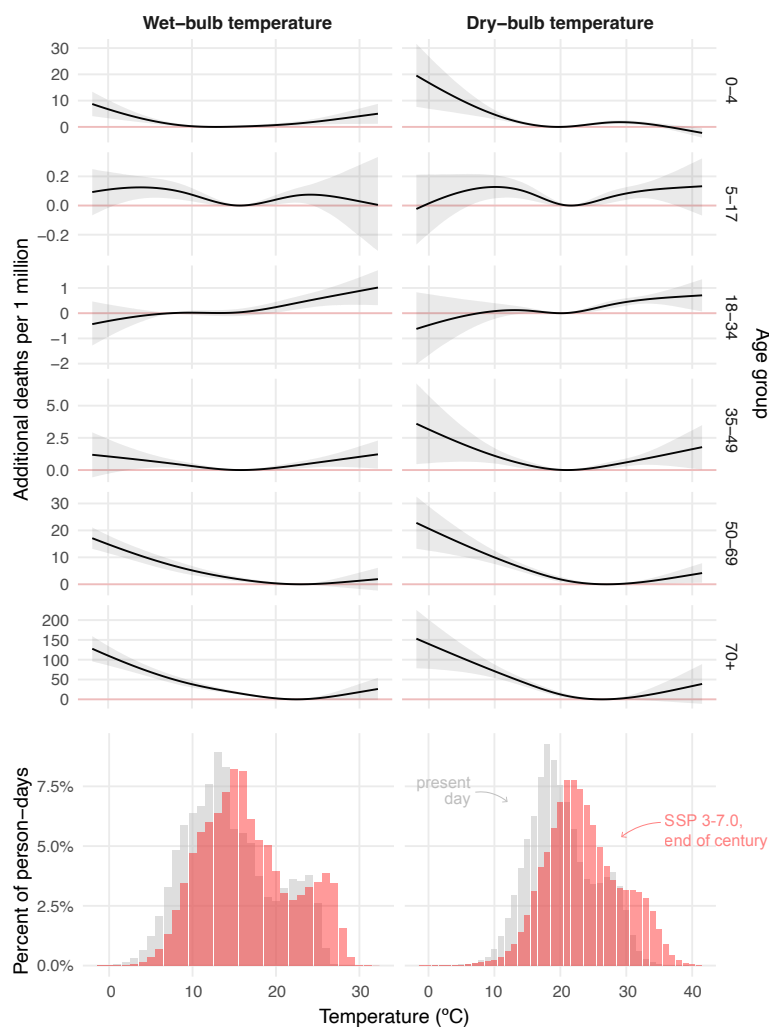


Figure S1: Relationships between mortality and exposure to wet- and dry-bulb temperature by age group in Mexico

This figure mirrors Figure 1, but expresses outcomes as absolute changes in deaths and adds a column for dry-bulb temperature. The top panels show the additional effects of 1 million person-days of exposure to the indicated daily average wet- and dry-bulb temperatures (x -axis) on mortality (y -axis); exposure and mortality are in terms of the indicated age group. Bands around each function indicate 95% confidence intervals. The bottom panel shows the distribution of daily average wet- and dry-bulb temperatures in Mexico throughout our sample period as well as the ensemble mean of projected temperatures under the SSP 3-7.0 emission scenario at the end of the century (2083–2099); we impose no change in population distribution or size.

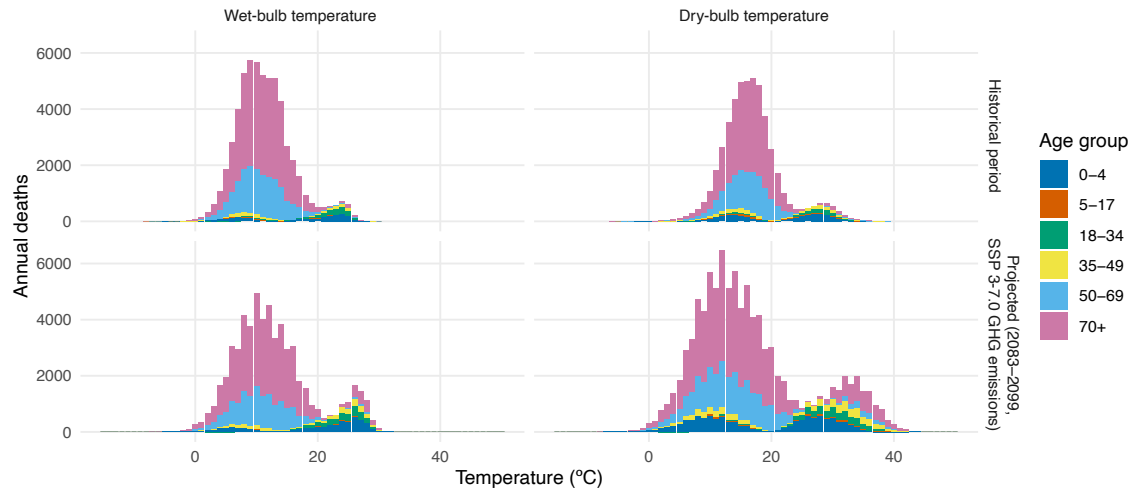


Figure S2: Historical and projected annual temperature-related deaths in Mexico for degree bins of wet- and dry-bulb temperature

This figure mirrors Figure 2, but adds a column for dry-bulb temperature. The panels show average annual temperature-related deaths resulting from exposure to days with the average wet- or dry-bulb temperatures shown on the x -axis during the historical period (top panels) and at the end of the century (2083–2099) under the SSP 3-7.0 emission scenario (bottom panels) across six age groups in Mexico. Projections assume that demographics, socioeconomic characteristics, and the population distribution remain fixed at their historical values. The figure shows mean projected deaths; see Figure S3 for projections with uncertainty.

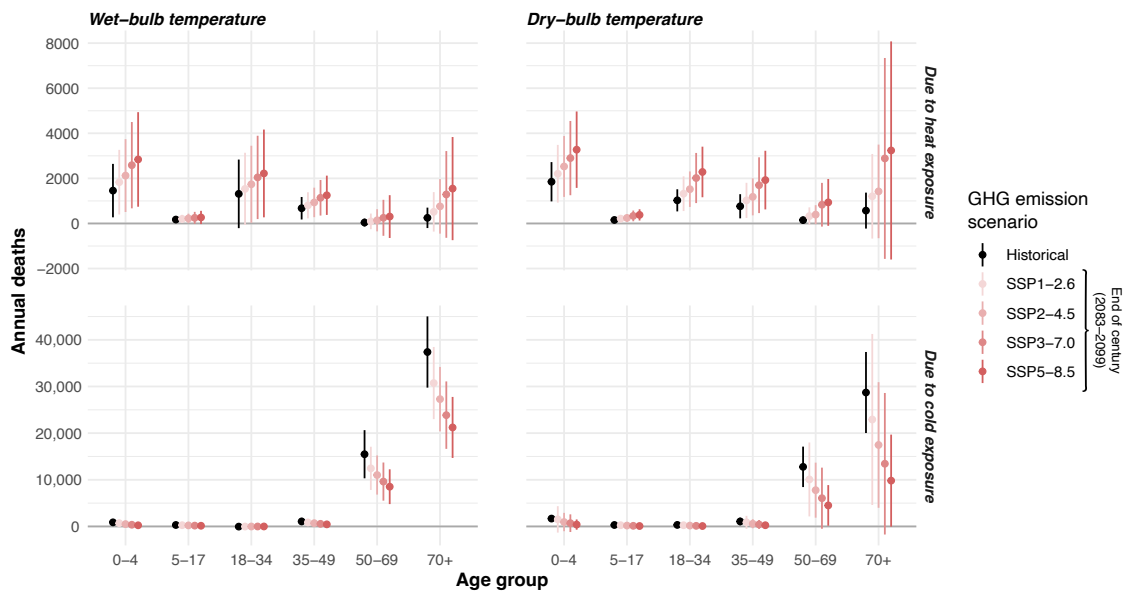


Figure S3: Historical and projected annual deaths due to heat and cold exposure by age group for wet- and dry-bulb temperature

This figure mirrors Figure 3, but adds a column for dry-bulb temperature. The figure depicts the annual number of deaths attributed to heat and cold exposure in Mexico historically and under temperatures prevailing at the end of the century in four greenhouse gas emission scenarios. Top panels indicate values for heat exposure, whereas bottom panels indicate values for cold exposure. Estimates using wet-bulb temperature are shown in the left panels, whereas those derived using dry-bulb temperature are shown in the right panels. Whiskers above and below each estimate depict 95% confidence intervals net of both econometric and climate uncertainty. Note that the range of the y -axis in the bottom panels is roughly five times the range of the y -axis in the top panels.

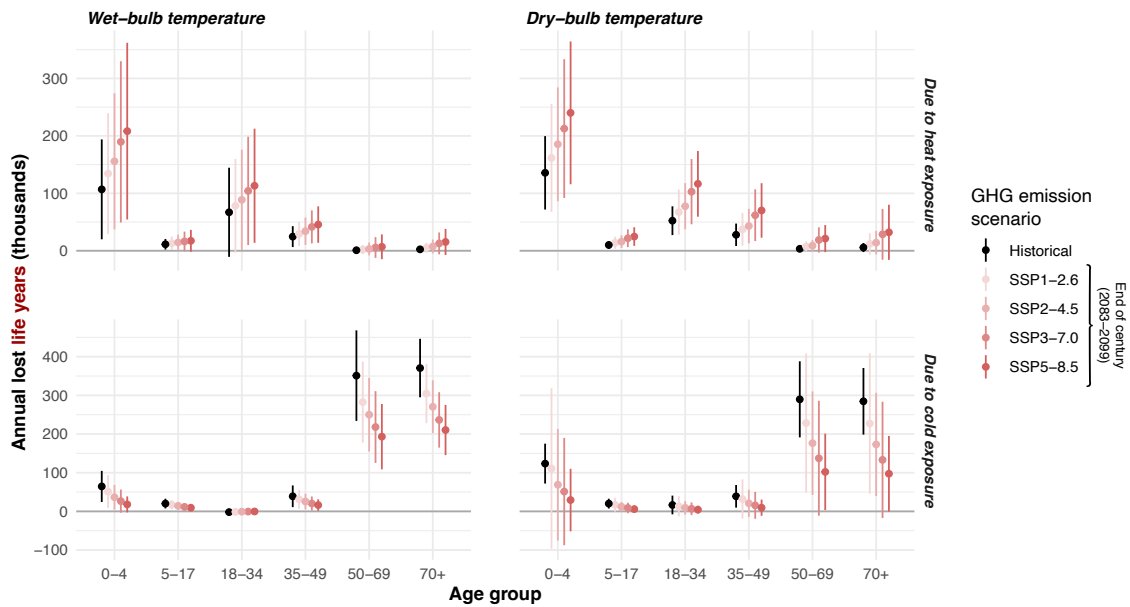


Figure S4: Historical and projected annual lost life years due to heat and cold exposure by age group for wet- and dry-bulb temperature

This figure mirrors Figure 4, but with the outcome as lost life years, rather than deaths. Potential remaining life years are taken from the UN World Population Prospects 2022, and are aggregated to time-invariant age group values by taking a population-weighted average across single age bins and years. The figure depicts the annual number of lost life years attributed to heat and cold exposure in Mexico historically and under temperatures prevailing at the end of the century in four greenhouse gas emission scenarios. Top panels indicate values for heat exposure, whereas bottom panels indicate values for cold exposure. Estimates using wet-bulb temperature are shown in the left panels, whereas those derived using dry-bulb temperature are shown in the right panels. Whiskers above and below each estimate depict 95% confidence intervals net of both econometric and climate uncertainty.

Distribution of proportion of impacts accruing to individuals under 35 years old

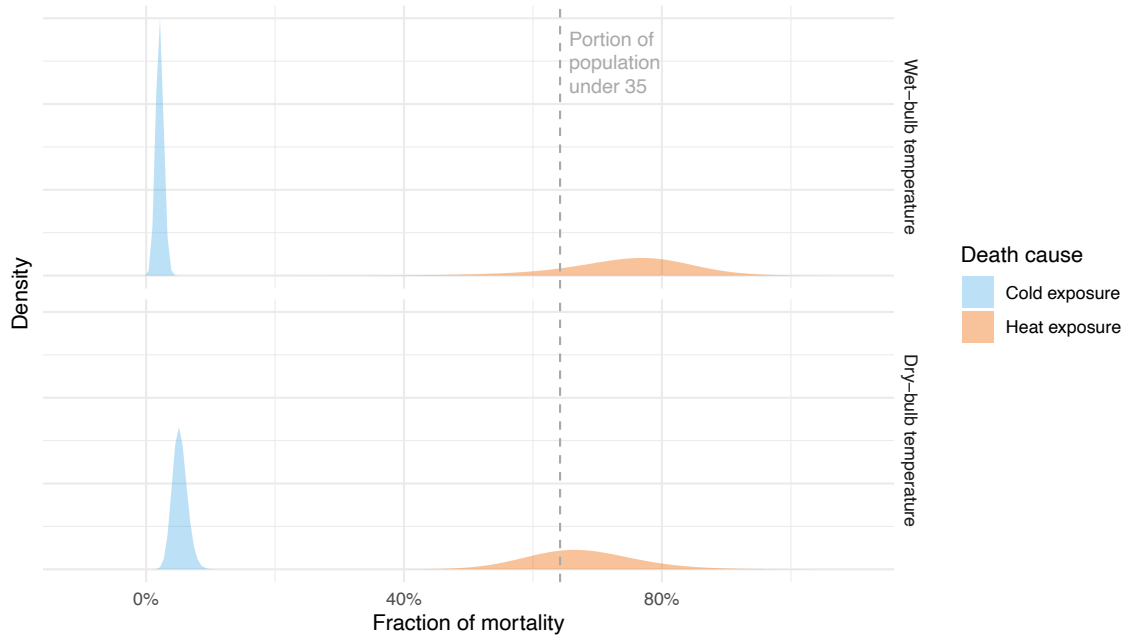


Figure S5: Distribution of estimates of the historical proportion of heat and cold-related deaths occurring to individuals under 35 years old.

Distributions depict the density of bootstrap samples i of $\frac{\text{deaths_under_35}_{i,\text{type}}}{\text{all_deaths}_{i,\text{type}}}$, where the number of samples is 10,000 and $\text{type} \in \{\text{cold-related}, \text{heat-related}\}$. Results using wet-bulb temperature are shown in the top panel, whereas results using dry-bulb temperature are shown in the bottom panel. As of the 2010 Census, around 63% of the Mexican population is under 35, a value labeled on the plot with a dashed vertical line.

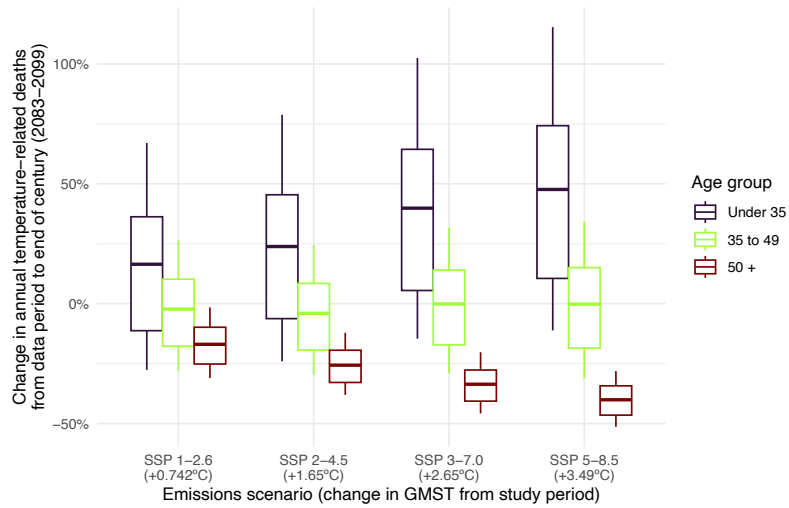


Figure S6: Projected percent change in annual deaths in Mexico under different climate change scenarios using wet-bulb temperature projections

The figure shows the percent change in average annual deaths by end-of-century (2083–2099) relative to the historical period for four different climate scenarios, indicated on the *x*-axis, and for three different age groups: those under 35 years old, between 35 and 49 years old, and over 50 years old. Box boundaries depict the 25th and 75th percentile of bootstrap estimates, while whiskers depict the 10th and 90th percentiles. Projections assume that demographics, socioeconomic characteristics, and the population distribution remain fixed at their historical values. The differences in levels is shown in Figure S7.

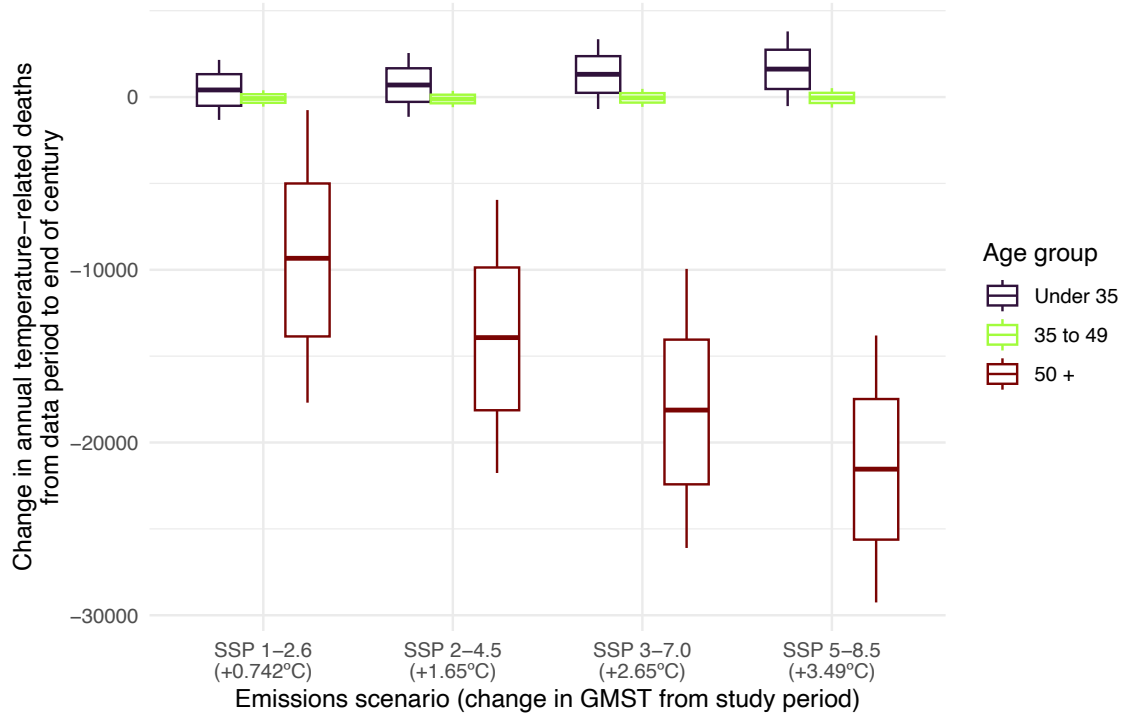


Figure S7: Projected change in annual deaths in Mexico under different climate change scenarios using wet-bulb temperature projections

The figure shows the level of average annual deaths by end-of-century (2083–2099) relative to the historical period for four different climate scenarios, indicated on the *x*-axis, for three different age groups: those under 35 years old, those between 35 and 49 years old, and those over 50 years old. Box boundaries depict the 25th and 75th percentile of bootstrap estimates, while whiskers depict the 10th and 90th percentiles. Projections assume that demographics, socioeconomic characteristics, and the population distribution remain fixed at their historical values. Figure S6 shows the same information but in terms of percent change.

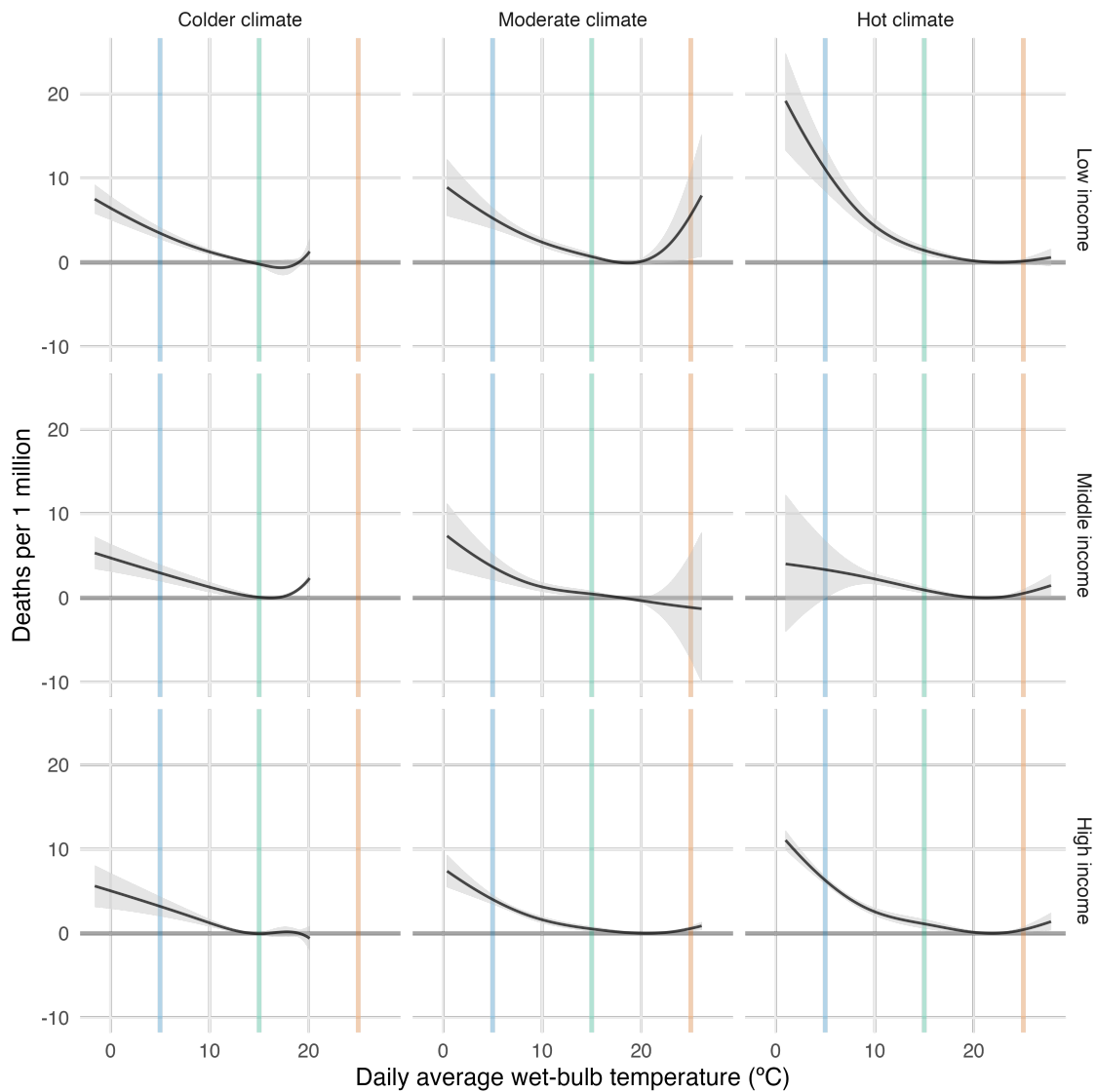


Figure S8: Heterogeneity in effects by climate and income tercile

Relationship between average daily wet-bulb temperature and additional deaths per 1 million person-days of exposure by income and climate tercile. Income terciles divide Mexico's municipalities into three roughly equal-population groups by their average earned income as reported by the Mexican census; climate terciles divide Mexico's municipalities into three roughly equal-population groups by their average annual wet-bulb temperature during the data period. Effects are for the overall population (pooled across age groups). Shaded area represents a confidence interval of 95%. Dose-response functions are shown to each tercile's population-weighted 0.01 and 99.99 percentile temperature exposure (colored vertical lines are added at 5, 15, and 25°C to aid visual comparison).

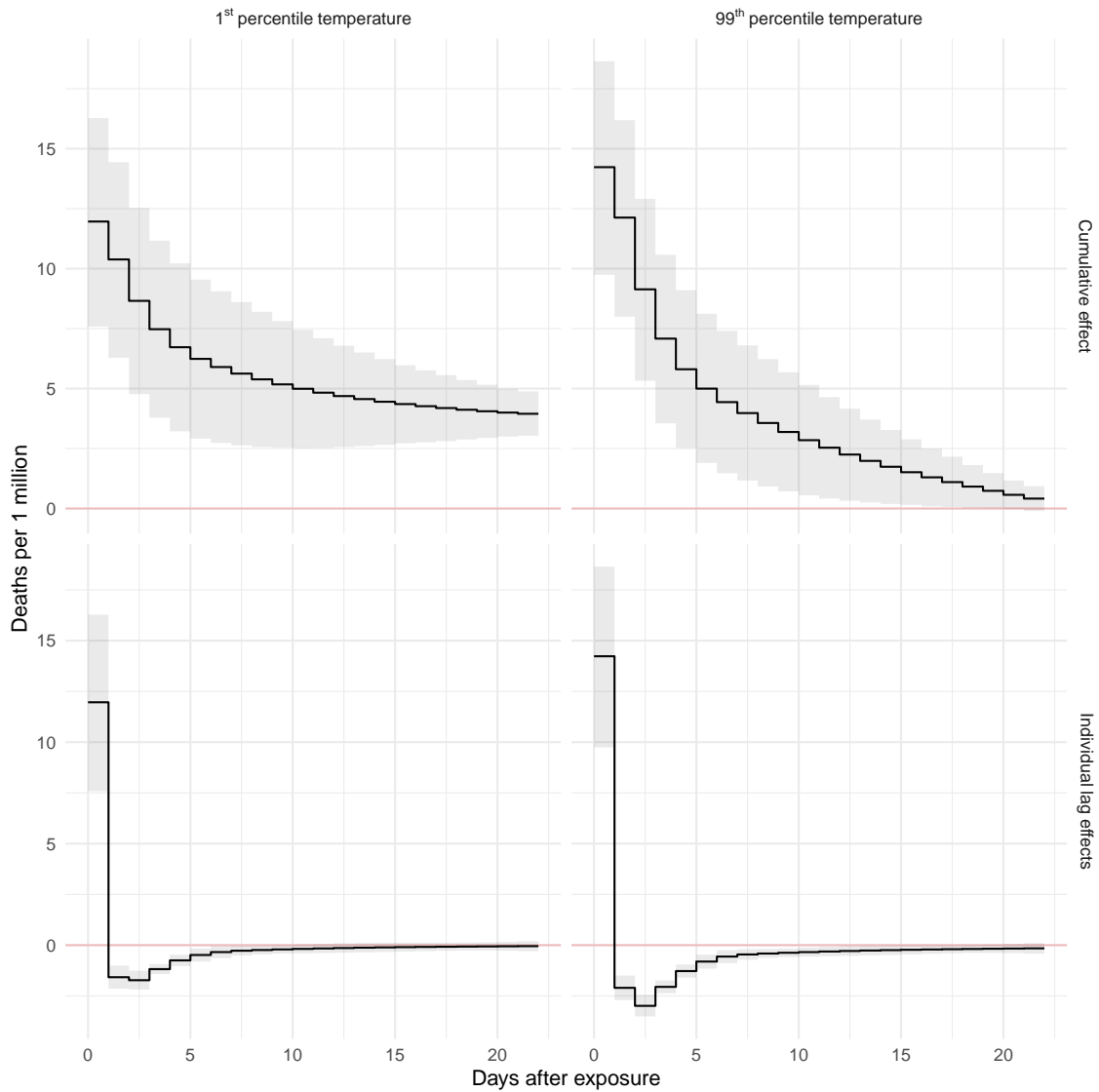


Figure S9: Lag-response relationship when estimating Eq. S-1

Additional deaths per 1 million person-days of exposure to average daily 1st- (left panels) and 99th- (right panels) percentile wet-bulb temperatures (approximately 3.96 and 25.25°C, respectively). Effects are for the overall population (pooled across age groups). Top panels show cumulative effects across the 21-day lag period; bottom panels show the effects at individual lags. Shaded area represents a confidence interval of 95%.

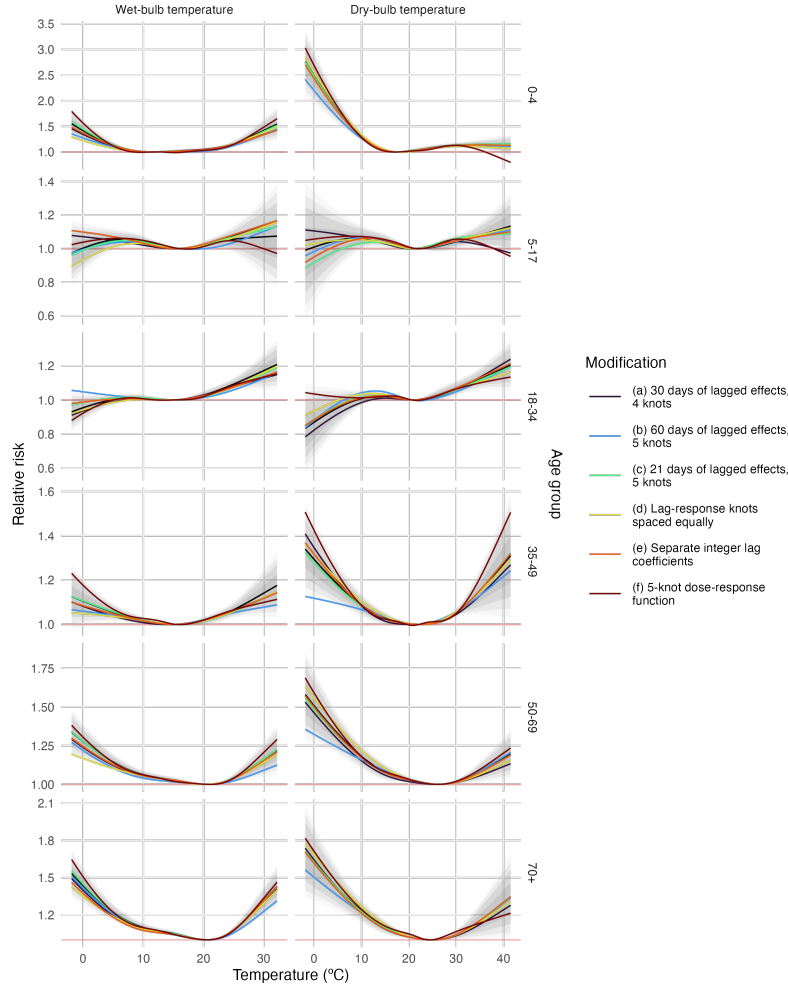


Figure S10: Robustness of results to modifications to Eq. S-1

Estimated relationship between wet- and dry-bulb temperature and relative risk of mortality by age group for alternate model specifications. (a) extends the main model’s 21-day lag period to 30 days and adds a single knot to the 3-knot lag–response specification to preserve a similar degree of flexibility in the lag–response function; (b) extends this further to 60 days and adds another knot to the lag–response function. (c) adds two additional knots to the main model’s 21-day lag structure, bringing the total number of lag–response function knots to five. (d) changes the placement of the main model’s three lag–response knots, placing them equally throughout the lag space instead of spaced logarithmically. (e) includes separate coefficients for each integer lag in the main model’s 21-day lag space. (f) changes the specification of the dose–response function, increasing the number of knots from three to five, with placement following [81]. Shaded bands around the main model (black line) result indicate 95, 90, 80, and 50% confidence intervals. Note that to reduce computational complexity with long-lag models, all models in this figure use state by week fixed effects rather than the state by day-of-year spline in the model in the body of the paper.

Table S1: Additional deaths per 1 million person–days of exposure to an average daily wet-bulb temperature in the indicated bin. Values were determined by estimating Equation S-1, but with a discretized version of the nonlinear dose–response component of $f_a(\cdot)$. Standard errors are shown in parentheses.

Temperature (°C)	Age group					
	0–4	5–17	18–34	35–49	50–69	70+
<3	2.923 (0.91)	0.057 (0.101)	-0.661 (0.178)	0.315 (0.385)	5.366 (1.255)	49.42 (9.21)
[3,6)	1.582 (0.504)	0.051 (0.041)	0.142 (0.077)	0.851 (0.194)	4.466 (0.83)	32.834 (6.13)
[6,9)	0.334 (0.327)	0.063 (0.033)	0.029 (0.044)	0.165 (0.134)	2.352 (0.581)	18.623 (3.643)
[9,12)	0.124 (0.218)	0.041 (0.026)	0.042 (0.037)	0.217 (0.101)	1.546 (0.37)	10.819 (2.361)
[12,15)	0.222 (0.216)	0.015 (0.027)	0 (0)	0.059 (0.088)	0.932 (0.369)	8.927 (2.212)
[15,18)	0 (0)	0 (0)	0.032 (0.053)	0 (0)	0.449 (0.286)	1.946 (1.353)
[18,21)	0.444 (0.208)	0.024 (0.022)	0.069 (0.067)	0.086 (0.09)	0 (0)	0 (0)
[21,24)	0.648 (0.22)	0.048 (0.024)	0.218 (0.071)	0.331 (0.114)	0.114 (0.227)	0.804 (1.062)
[24,27)	1.441 (0.307)	0.058 (0.045)	0.303 (0.083)	0.483 (0.148)	1.174 (0.488)	9.606 (2.47)
27+	3.392 (0.982)	0.008 (0.35)	1.049 (1.158)	2.061 (1.272)	3.575 (2.399)	41.039 (8.131)

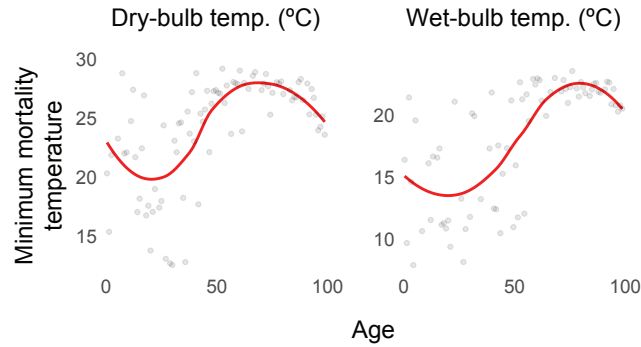


Figure S11: Minimum mortality temperatures across age groups in Mexico

This figure demonstrates the relationship between age and the temperature at which mortality is minimized (“MMT”). A locally-weighted regression line is added to aid in visual inspection, as these parameter estimates are subject to noise. These MMTs are determined by separately estimating Eq. S-1 for each age and temperature metric and determining the temperature at which mortality risk is minimized. MMT decreases from birth to the mid-20s, and then increases substantially with age to around age 70 before flattening and decreasing slightly to age 100. Individuals in their mid-20s have a dry-bulb MMT of 20°C and a wet-bulb MMT of 13°C. Dry-bulb MMT peaks at 28°C at age 70 and wet-bulb MMT peaks at 22°C at age 75.

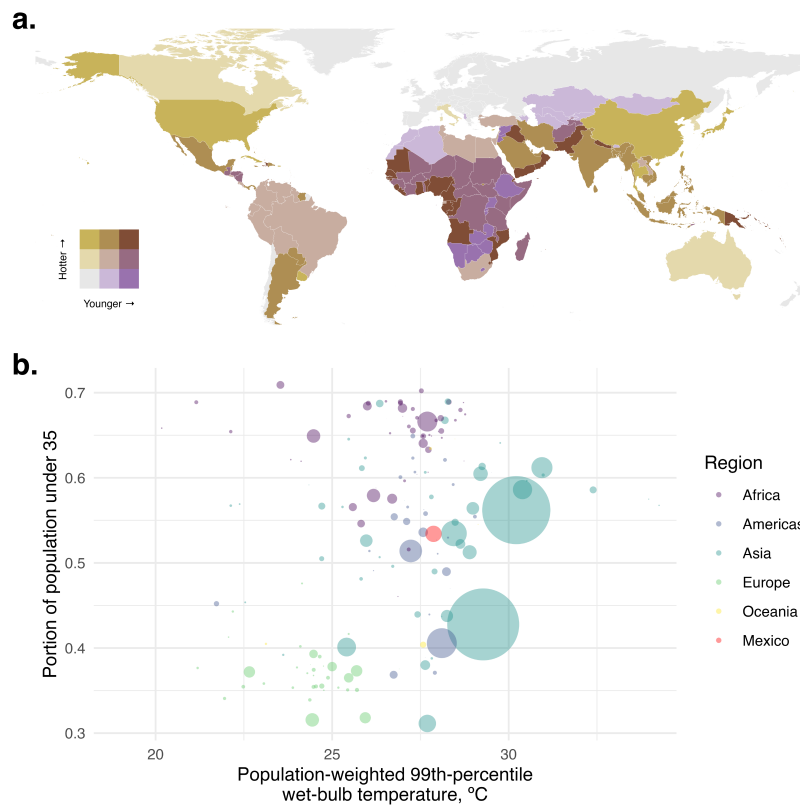


Figure S12: Historical extreme wet-bulb temperature exposures and current portion of population under 35

a. Countries colored according to their tercile of the global distribution of (1) historical extreme wet-bulb temperature exposures: 99th percentile of population-weighted exposures, with temperatures estimates by [32] using ERA-5 Interim values from 1979 to 2017 and population distribution information from [84] and (2) portion of 2010 population under 35 [70]. **b.** Scatterplot of country-level historical extreme wet-bulb temperature exposure and the portion of the 2010 population under 35. Points are scaled according to total population size.

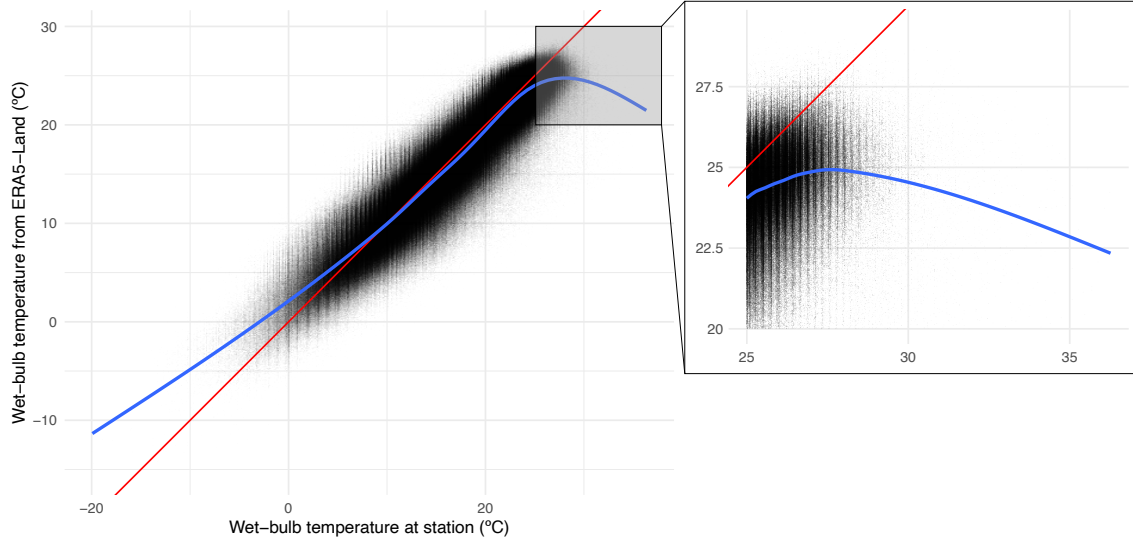


Figure S13: Daily average wet-bulb temperatures recorded at stations and in ERA5-Land

Data spans the period 1998–2019. Each point represents a pair of observations at a weather station (mean of sub-daily values) in Mexico and the corresponding value of ERA5-Land at that position and time (mean of hourly values). The blue line is a generalized additive model of cubic regression splines estimated by REML. The red line, for comparison, illustrates what would be observed with a one-to-one correspondence.

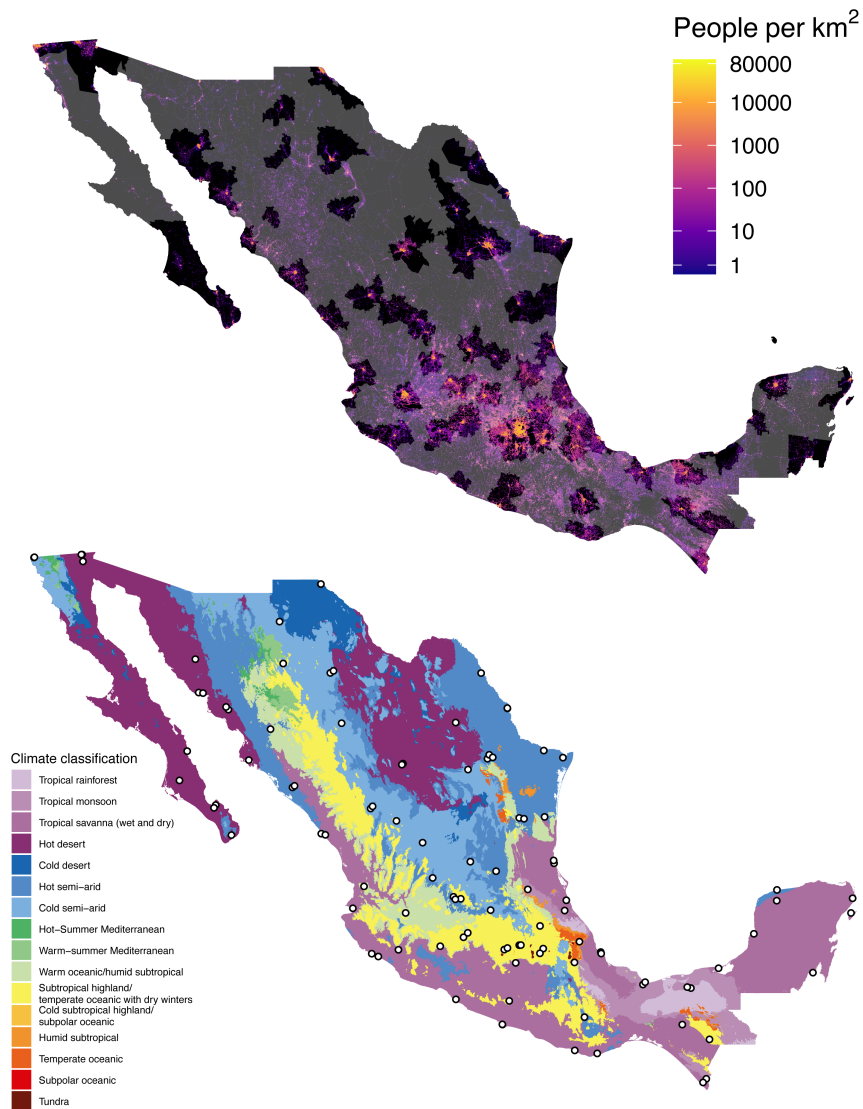


Figure S14: Map of population, municipalities, weather monitor locations, and climate zones in Mexico

The top panel of this figure shows the population density of Mexico (background color gradient) in the municipalities analyzed. The subset of municipalities dropped from our analysis (because they are too far from weather stations) are grayed out. The bottom panel of this figure shows the location of weather stations used in our analysis (white points with black outlines) and Köppen climate zones (background color gradient).